NTNU
Norwegian University of
Science and Technology

A new Design of a Francis Turbine in order to reduce Sediment Erosion

Hallvard Meland

Master of Science in Energy and Environment
Submission date: June 2010
Supervisor: Ole Gunnar Dahlhaug, EPT

Problem Description

Bakgrunn
Sanderosjon i Francis turbiner er et problem i områder der det er mosunperioder i verden. Dette gjelder særlig for Himalaya og Andes der det i tillegg er store mengder med kvarts i sedimentene. SN-Power har inverstert i flere kraftverk i Peru som er meget belastet med sedimenter i monsun perioden. Ved Cahua Krafttverk så er det to Francis turbiner som har en effekt på 44 MW til sammen. I disse turbinene så går det i ekstreme perioder opp til 50 kg/s med sedimenter gjennom hver av disse turbinene. Dette medfører at de må bytte ut deler av turbinen hvert eneste år. SN-Power ønsker å se nærmere på om det er mulig å lage et nytt design av turbinene ved Cahua Kraftverk som kan redusere sanderosjonen betraktelig.

Mål
Det skal designes en helt ny turbin ved Cahua Kraftverk som har redusert sanderosjonen med 30 50% i forhold til dagens turbin.

Oppgaven bearbeides ut fra følgende punkter:

1.   Studenten må gjennomføre literatursøk for å se hva som er state of the art innefor turbin design som er utsatt for sanderosjon.
2.   Studenten skal designe tromme, stag skovler, ledeapparat, løpehjul og sugerør på Cahua Kraftverk.
3.   Dersom det er tid skal gjennomføres CFD-analyse på deler av turbinen.

Assignment given: 01. February 2010
Supervisor: Ole Gunnar Dahlhaug, EPT

Norges teknisk-
naturvitenskapelige universitet
NTNU

Fakultet for ingeniørvitenskap og teknologi
Institutt for energi- og prosessteknikk

◧ NTNU

EPT-M-2010-43

MASTEROPPGAVE

for

Stud.techn. Hallvard Meland
Våren 2010

Nytt design av en Francisturbin for å redusere sanderosjon
New design of a Francis turbine in order to reduce sediment ersion

Bakgrunn
Sanderosjon i Francisturbiner er et problem i områder der det er mosunperioder i verden.
Dette gjelder særlig for Himalaya og Andes der det i tillegg er store mengder med kvarts i
sedimentene. SN-Power har inverstert i flere kraftverk i Peru som er meget belastet med
sedimenter i monsunperioden. Ved Cahua Krafttverk så er det to Francisturbiner som har en
effekt på 44 MW til sammen. I disse turbinene så går det i ekstreme perioder opp til 50 kg/s
med sedimenter gjennom hver av disse turbinene. Dette medfører at de må bytte ut deler av
turbinen hvert eneste år. SN-Power ønsker å se nærmere på om det er mulig å lage et nytt
design av turbinene ved Cahua Kraftverk som kan redusere sanderosjonen betraktelig.

Mål
Det skal designes en helt ny turbin ved Cahua Kraftverk som har redusert sanderosjonen med
30 – 50 % i forhold til dagens turbin.

Oppgaven bearbeides ut fra følgende punkter:

1. Studenten må gjennomføre literatursøk for å se hva som er "state of the art" innefor
   turbin design som er utsatt for sanderosjon.
2. Studenten skal designe tromme, stag skovler, ledeapparat, løpehjul og sugerør på
   Cahua Kraftverk.
3. Dersom det er tid skal gjennomføres CFD-analyse på deler av turbinen.

---- " ---

Senest 14 dager etter utlevering av oppgaven skal kandidaten levere/sende instituttet en detaljert fremdrift- og eventuelt forsøksplan for oppgaven til evaluering og eventuelt diskusjon med faglig ansvarlig/veiledere. Detaljer ved eventuell utførelse av dataprogrammer skal avtales nærmere i samråd med faglig ansvarlig.

Besvarelsen redigeres mest mulig som en forskningsrapport med et sammendrag både på norsk og engelsk, konklusjon, litteraturliste, innholdsfortegnelse etc. Ved utarbeidelsen av teksten skal kandidaten legge vekt på å gjøre teksten oversiktlig og velskrevet. Med henblikk på lesning av besvarelsen er det viktig at de nødvendige henvisninger for korresponderende steder i tekst, tabeller og figurer anføres på begge steder. Ved bedømmelsen legges det stor vekt på at resultatene er grundig bearbeidet, at de oppstilles tabellarisk og/eller grafisk på en oversiktlig måte, og at de er diskutert utførlig.

Alle benyttede kilder, også muntlige opplysninger, skal oppgis på fullstendig måte. For tidsskrifter og bøker oppgis forfatter, tittel, årgang, sidetall og eventuelt figurnummer.
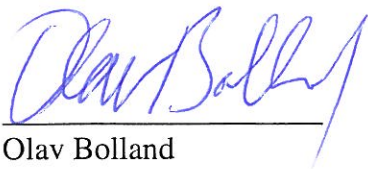
Det forutsettes at kandidaten tar initiativ til og holder nødvendig kontakt med faglærer og veileder(e). Kandidaten skal rette seg etter de reglementer og retningslinjer som gjelder ved alle (andre) fagmiljøer som kandidaten har kontakt med gjennom sin utførelse av oppgaven, samt etter eventuelle pålegg fra Institutt for energi- og prosessteknikk.

I henhold til "Utfyllende regler til studieforskriften for teknologistudiet/sivilingeniørstudiet" ved NTNU § 20, forbeholder instituttet seg retten til å benytte alle resultater og data til undervisnings- og forskningsformål, samt til fremtidige publikasjoner.
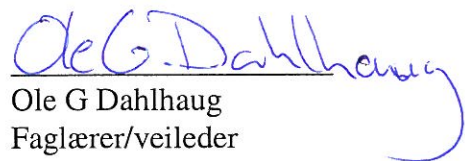
Ett -1 komplett eksemplar av originalbesvarelsen av oppgaven skal innleveres til samme adressat som den ble utlevert fra. Det skal medfølge et konsentrert sammendrag på maksimalt én maskinskrevet side med dobbel linjeavstand med forfatternavn og oppgavetittel for evt. referering i tidsskrifter).

Til Instituttet innleveres to - 2 komplette kopier av besvarelsen. Ytterligere kopier til eventuelle medveiledere/oppgavegivere skal avtales med, og eventuelt leveres direkte til de respektive. Til instituttet innleveres også en komplett kopi (inkl. konsentrerte sammendrag) på CD-ROM i Word-format eller tilsvarende.

NTNU, Institutt for energi- og prosessteknikk, 12. januar 2010

Olav Bolland
Instituttleder

Ole G Dahlhaug
Faglærer/veileder

Medveileder:
Torbjørn Nielsen

Preface

This report is the master thesis written by Hallvard Meland, at the water power laboratory at NTNU, during the spring semester 2010. Professor Ole Gunnar Dahlhaug has been the supervisor of this thesis, and Biraj Singh Thapa at Katmandu University has been an allied, working on the same subject.

The topic of this thesis is to design a new type of Francis turbines in order to reduce sediment erosion. The goal has been to reduce the erosion with 30 to 50 percent. As a test case, Jhimruk power plant in Nepal has been chosen.

I want to thank Professor Ole Gunnar Dahlhaug for his guiding throughout this period. This has been both inspiring and very useful. I also want to thank Mette Eltvik from the Water Power Laboratory and Ola Thorvaldsen from DynaVec AS for helping me with the CFD-analysis. This has saved me from wasting a lot of time. At last I want to thank Biraj Singh Thapa for guiding me around at Katmandu University. This was a very inspiring experience for me, and left me with the feeling that the outcome of this kind of research can help countries dealing with sediment erosion to utilize their water power potential.

Hallvard Meland
25.06.2010

Abstract

This Master Thesis is about the sand erosion challenges with the Francis turbines. The background for studying this subject is the fact that the sand erosion problem is a very negative factor for the development of new hydro electric power plants in many developing countries. The target with this Master Thesis has been to develop a new design, a revised version of the Francis turbine, reducing the sand erosion by 30- 50 per cent compared with today´s version of turbines.

The present version of Francis turbines is consisting of three different vane cascades, The stay, guide and runner cascade. The sand erosion is in proportion with the relative speed between the sand particles and the steel cubed. This challenge has thus been analyzed and solved by reducing this speed through the turbine.

Regarding the stay vanes, a new design has been proposed where the stay vanes are pressing the spiral casing from outside and not from the inside. This will result in the fact that the whole sand erosion problem has been removed.

It has been proposed to remove the the guide vane cascade. This will consequently remove the sand erosion problem here as well. A favourable solution is to increase the reaction degree.

For the runner a study of four different parameters has been carried out. These parameters were the number of pole pair in the generator, outlet angle, reaction degree and UCu distribution. The analysis shows that a reduction of sand erosion at the runner outlet was possible by selecting a higher number of pole pair along with a higher outlet angle than what is standard practice today. This result is of high significant importance since the sand erosion is biggest at the runner outlet. A change in the reaction

degree may enable the erosion at the inlet of the runner, whereas a change in the UcU will change the erosion between the inlet and outlet. By selecting favourable parameter values, a substantial reduction of sand erosion in a Francis turbine will be possible.

The turbines in this Master thesis have been designed in the computer program Matlab. A proposal for new design based upon the results of the parameter study has been analyzed in a CDF analysis. This analysis has been made in Ansys CFX.

Sammendrag

Denne masteroppgaven omhandler sanderosjonsproblematikken i Francis-turbiner. Bakgrunnen for å studere dette fagfeltet er at sanderosjonsprob-lemet er med på å hemme utbygging av vannkraftverk i mange u-land. Målsetningen med oppgaven har vært å komme opp med et nytt design, en revidert type Francisturbin, som reduserer sanderosjon med 30 til 50 pros-ent iforhold til dagens turbiner.

Dagens Francisturbiner består av tre forskjellige sett med skovler, hen-holdsvis stagskovler, løpeskovler og ledeapparatet. Sanderosjon er pro-posjonal med den relative farten mellom sandpartiklene og stålet i tredje potens. Problemstillingen har dermed blitt forsøkt løst ved å redusere denne farten igjennom turbinen.

Når det gjelder stagskovlene, har det blitt foreslått et design hvor skov-lene presser spiraltromma sammen fra yttersiden og ikke innsiden. Dette vil gjøre at hele sanderosjonsproblematikken forsvinner.

Det er foreslått å ta bort ledeapparatet. Dette vil fjerne sanderosjonsprob-lemet også her. Det er også sett på hvordan forskjellige parametere kan variere sand erosjonen i ledeapparatet. En gunstig løsning er å øke reak-sjonsgraden.

For løpehjulet har det blitt utført et parameterstudie av fire forskjellige pa-rametere. Parametrene var antall polpar i generatoren, utløpsvinkel, reak-sjonsgrad og UCu fordeling. Studiet viste at det var mulig å redusere erosjo-nen på utløpet ved å velge et høyere poltall samt en høyere utløpsvinkel enn det som er vanlig praksis i dag. Dette resultatet er av stor betydning da det er ved utløpet at sanderosjonen er størst. En endring i reaksjonsgrad vil kunne endre erosjonen ved innløpet av løpehjulet, mens en endring i UcU fordeling vil endre erosjonen imellom inn og utløp. Ved å velge gunstige parameterverdier vil det være mulig å kraftig redusere sanderosjonen i en Francisturbin.

Turbinene i denne oppgaven har blitt designet i dataprogrammet Matlab. Et forslag til design basert på resultatene av parameterstudiet har blitt analysert i en CFD-analyse. Analysen er gjort i Ansys CFX.

Contents

List of symbols and abbreviations

Symbols

Term	Symbol	Unit
Reaction degree	R	-
Efficiency	η	-
Velocity of runner	U	m/s
Absolute velocity	C	m/s
Relative velocity	w	m/s
Rotational speed	n	rpm
Number of poles	Z	-
Diameter	D	m
Radius	R	m
Length of vanes	L	m
Angle between U and w	β	rad
Angle between U and C	α	rad
Height at runner inlet	B	m
Force	F	N
Pressure	P	Pa
Torque	T	Nm
Effect	P	W
Angular frequency	ω	rad/s
Length of streamline in the axial view	ΔG	m
Length of streamline in the radial view	ΔH	m
Number of vanes	N	-
Constant of gravity	g	m/s^2
Thickness	t	m
Density of mass	ρ	kg/m^3
Flow rate	Q	m^3/s
Head	H	m
Friction factor	f	-
Area	A	m^2
Perimeter	P	m

Table 1: List of symbols

Indexes

Term	Symbol
Runner inlet	1
Runner outlet	2
Reduced values	underline
Radial	u
Meridional	m
Hydraulic	h
Time derivative	$\cdot$
Guide vane	gv
Stay vane	sv
Inlet	i
Outlet	o
Initial axis	axf
Effective	e
Friction	f

Table 2: List of indexes

Abbreviations

NTNU - Norges Tekniske Naturvitenskaplige Universitet
BTI - Butwal Technical Institute
MW - Mega Watt
IEC - The International Electrotechnical Commission
rpm - revolutions per minute

List of Figures

4

List of Tables

Chapter 1

Introduction

Because of its location in the Himalayas, Nepal is blessed with a huge water power potential. According to [Tha10], Nepal has a total potential of 83000 MW, where about 43000 MW is economically feasible. Despite of this, only about 550 MW has been buildt [Tha10]. One of the major reasons for this low installed effect is due to the severe sediment erosion problem. This means that the development of a new type of turbines, that can handle the high sediment rates, is extremely important. If successful, this can lead to a significant increase in water power production in Nepal. This can have a huge impact on both the country's economy and living standard. This statement can be confirmed by [Bla07], which states that economic growth in the long run, only can be caused by technological development. The reasoning above is valid for other countries than Nepal. Typically, countries in mountain chains with monsoon periods often have sediment erosion problems. Besides the Himalayas, the Andes in South-America and the Rocky Mountains in North-America are good examples.

As mentioned in the preface, Jhimruk power plant in Nepal is the test case of this thesis. This is a power plant built by the Norwegian engineer Odd Hoftun, in cooperation with Butwal Technical Institute, BTI. The power plant has three Francis turbines, equal in size. The results will there-

fore hold for all three turbines. In the result, discussion and conclusion, today's runner serves as the reference runner. Of course the changes made in the design at Jhimruk will also tend to have the same effects in other power plants around the world.

The theory chapter consists of three main parts. The first part is the turbine design algorithm. The second part is the sediment erosion part. Here Tsuguo's model for sand erosion is presented, and some theory of how to reduce the relative velocity in different parts of the runner is presented. These are basically three theses that I myself have derived when working with this subject. It contains an equation for optimal reaction degree, optimal outlet diameter and optimal UCu distribution through the runner. The word optimal here means where the parameter gives the lowest relative velocity. This does not mean that it is the optimal parameter value when considering the whole picture, only that it is the parameter value where the relative velocity at the specified place is lowest. Since the sediment erosion is highly related to velocity, this value can be seen as optimal with regards to sediment erosion, and therefore the optimal notation is used. The last part of the theory chapter is about friction loss in the turbine. This is included because the friction loss in the different turbines tested is presented in the result part and discussed in the discussion part.

Chapter 2

Literature Review

2.1 What research is done to prevent sediment erosion?

The research whose aim is to address sediment erosion in water power plants can be separated in different parts. One area of research is to develop techniques that will reduce the amount of sediments in the water before it enters the hydraulic machinery. Another approach is to look at the choice of turbine materials. A solution offered from this approach is to coat the turbine with a hard material, and thereby increasing the turbines durability. The third method, as done in this thesis, looks into how different turbine designs will change the erosion. This approach is often conducted by turbine suppliers, but they don't seem to reveal their secrets. This means that it is difficult to know how much of the findings in this thesis that is already known for turbine suppliers around the globe. At universities, research trying to understand the nature of sediment erosion is conducted.

2.1.1 Techniques that reduce the amount of sediments

One way to reduce the sediment erosion is to reduce the amount of particles. The author of this thesis was during this study in Nepal, where he was given

a tour around at HydoLab in Kathmandu. They are trying to reduce the amount of sediments before they reach the turbine. According to them, this can be done by applying some kind of pools in which the water will stay for some time. During this time, the sediments will, due to gravity, tend to drop against the bottom. The result is that the water above has a smaller concentration of sediments. One problem with this approach, is the fact that the particles are so small that is takes long time for the gravity to bring the sediments down to the bottom of the water.

2.1.2 Choice of turbine materials

As mentioned, it is possible to cover the turbine with a coating. This will add durability to the turbine, and thereby increase its endurance in sediment laden waters. DynaVec AS from Norway has tested their coated turbine in rough conditions at Cahua power plant in Peru with very good results [Dah]. They use a ceramic coating, which makes the turbine surface harder. [Pre] states that the following various coatings have been developed: Hard Chrome plating, Plasma nitriding, Boronising and HVOF coating.

2.1.3 Research of sediment erosion nature

The aim of this research is to understand what kind of parameters that affects the sediment erosion. Over the years many scientists have come up with their equations and theory that describes erosion behavior. Three of these equations are shown later in this literature review. The general finding from this kind of research is that the erosion parameters can be classified in different groups. The groups are; the parameters of the sediment particles, the parameters of the turbine and operating conditions.

2.2 Sediment Erosion Theory

According to Bhushan 2002, the removal of solid material from rubbing surfaces can be classified into six different wear mechanisms. However, in

this thesis, only abrasive and erosive wear will be of interest.

2.2.1 Abrasive wear

Abrasive wear is wear coursed by particles traveling over a surface. In order to create damage, it is enough that the abrasive particle has a hardness of 0,83 compared to the surface hardness. When the ratio becomes larger than 1,2, rapid abrasive wear can occur. The abrasive wear is further distinguished into four different mechanisms, see figure 2.1.
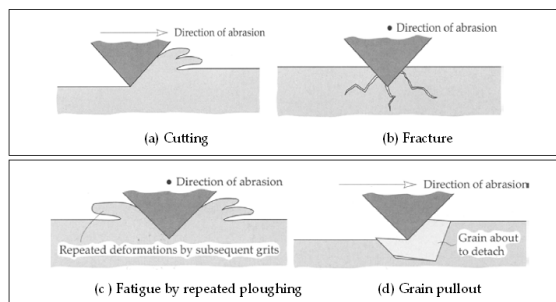
Figure 2.1: Mechanisms of abrasive wear[Neo10]

The illustration 2.1 part a, shows the classical model of abrasive mechanism, a particle cutting the surface along its way. If the surface material is brittle, fracture of the surface may occur as shown in figure b. If the surface is ductile, it will rather deform than some of the material being cut away. This is illustrated in figure c. The mechanism illustrated in figure d, shows a grain of the surface material being pulled out. The mechanism is therefore called pullout.

2.2.2 Erosive wear

Also erosive wear is divided into four different mechanisms, as seen in figure 2.2.
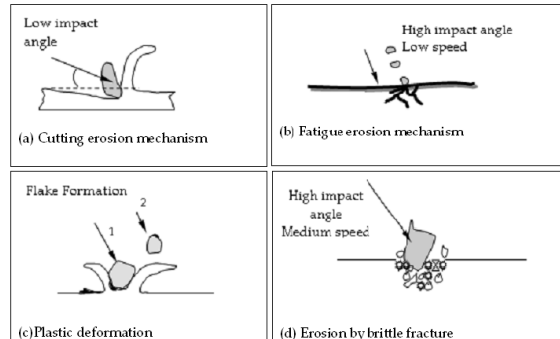
Figure 2.2: Mechanisms of erosive wear[Neo10]

If the particle hits the surface at a low impact angle as in illustration-a, the mechanism is called abrasive erosion.
(b) If particles hit the surface at a high impact angle, the most likely outcome is tendencies of fatigue and crack development of the surface.
(c) If the surface is ductile and the impact angle is high, the deformation shown in illustration c can occur. After repeated hitting, the deformation grains can detach as debris.
(d) When the particles hitting the surface are sharp, the erosion will be governed by brittle fracture.

2.2.3 IEC's Sediment Erosion Equation

The International Electrotechnical Commission has made a guide for dealing with abrasive erosion in hydraulic machines. This guide gives a very good decription of the different parameters that will change the magnitude of the sediment erosion. The parameters are listed in the table under, and the equation they have proposed is equation 2.1.

- f(Particle velocity)=(particle velocity)^n
  [IEC09] suggests to use n=3. However it is important to remember that different literature use different values for n. The range is

normally between 2 and 4. The fact that the abrasion rate is proportional to the particle velocity cubed indicates that this parameter is extremely important. Because of the assumption made in this thesis, that the particles follow the water flow, this velocity correspond to the relative velocity between the water and the steel in the runner, and the waters absolute velocity in both the stay and guide vanes.

- f(Particle concentration)=C
  The total weight of all solid particles in one m^3 of water.

- f(particle properties, turbine material properties)=$K_{hardness}$
  This parameter represents the hardness of the particles relative to the turbine material.

- f(flow pattern)=K_f
  This constant is there to describe the flow patterns of each part of the turbine. It reflects flow turbulence, impingement angle curvature radius, etc.

- f(particle size)=K_{size}
  Factor that describes how the abrasion relates to the size of the particles.

- f(particle shape)=K_{shape}
  Factor that describes how the abrasion relates to the shape of the particles.

- f(turbine material properties)=K_m
  Factor that describes how the abrasion relates to the properties of the turbine material.

When combining these different functions, an expression for the abrasion depth is found.

$$\frac{dS}{dt} = w^3 \cdot K_{hardness} \cdot C \cdot K_{shape} \cdot K_{size} \cdot K_f \cdot K_m \ [\text{thickness/time}] \quad (2.1)$$

2.2.4 Tsuguo's sediment erosion equation

In 1999, Tsuguo made a sediment erosion equation based on 8 years of data from 18 different hydro power plants [Neo10]. This is the equation used in this thesis to determine the sediment erosion.

$$W = \lambda \cdot c^x \cdot a^y \cdot k_1 \cdot k_2 \cdot k_3 \cdot V_{Char}^Z \qquad \text{[m]} \qquad (2.2)$$

where, W is the loss of thickness per unit time.
λ is the turbine coefficient.
a is the average sediment size based on a unit value.
$k_1 and k_2$ are shape and hardness coefficient of the sediments.
k_3 is the abrasion resistant coefficient of the turbine material.

In cooperation with Hari Prasad Neopane, the product of the constants in equation 2.2 are in this thesis equal to 0,3.

When dealing with erosion in hydro turbines, it is difficult to change the properties of the particle itself, but we can try to reduce the relative velocity between the surfaces and the water. This is exactly what has been done in this study.

2.2.5 Tabakoff's sediment erosion equation

The erosion model used by the Ansys CFX-solver in the CFD part is the model of Tabakoff. Equation 2.3 describes the model.

$$E = k_1 \cdot f(\gamma) V_P^2 \cdot \cos^2 \gamma \cdot \left(1 - R_T^2\right) + f(V_{PN}) \qquad (2.3)$$

Where:

$$f(\gamma) = \left(1 + k_2 \cdot k_{12} \cdot \sin \gamma \frac{\pi/2}{\gamma_0}\right)^2 \qquad (2.4)$$

$$R_T = 1 - k_4 \cdot V_P \cdot \sin \gamma \qquad (2.5)$$

$$f(V_{PN}) = k_3 \cdot (V_P \cdot + sin\gamma)^4 \qquad (2.6)$$

$$K_2 = \begin{cases} 1,0 & \text{if} \quad \gamma \leq 2\gamma_0 \\ 0,0 & \text{if} \quad \gamma > 0 \end{cases}$$

E is Tabakoff's measure of erosion, which is the eroded wall material divided by the mass of the particles.

V_P is the relative velocity between the wall and the particle at impact.

γ is the angle between the wall and the particle at impact in radians.

γ_0 is the impact angle that gives maximum erosion.

k one to three are constants determent by the combination of wall material and particle.

Chapter 3

Turbine design theory

3.1 Main dimensions

To start designing a Francis turbine, the main dimensions have to be calculated. In order to do so, some of the parameters are empirical. The ordinary procedure is to first calculate the number of pool pairs which is natural. However in this thesis, the number of pools need to be considered with regard to sand erosion. The following algorithm is the one used in this thesis, calculating the main dimensions from six parameters. These obviously include the head and the volume flow rate, which is kept constant, but also the efficiency degree of the turbine. The three remaining parameters are the reaction degree, the outlet angel and the number of pool pairs in the generator.

3.1.1 Reaction degree

The reaction degree is the fraction of pressure energy the turbine converts into mechanical energy from the total energy transformation. The transformation of energy comes either from pressure energy or velocity energy. Mathematically the reaction degree can be described as[Elt09]

$$R = 2\underline{U_1} \cdot \underline{C_{u1}} - \underline{C_{u1}^2} \qquad [\text{-}] \qquad (3.1)$$

Euler's turbine equation states that

$$\eta_h = 2\ \left(\underline{U_1} \cdot \underline{C_{u1}} - \underline{U_2} \cdot \underline{C_{u2}}\right) \qquad \text{[-]} \qquad\qquad (3.2)$$

To avoid a swirl in the draft tube the design criteria is that C_{u2} equals zero. When combining the two equations above, the following equation is derived.

$$\underline{C_{u1}^2} = \eta_h - R \qquad \text{[-]} \qquad\qquad (3.3)$$

From 3.3 we see that that the reaction degree will determine the reduced inlet velocity. More pressure energy into the turbine will mean less velocity energy input, in other words a reduced C_{u1} compared to U_1. In this way the reaction degree will together with C_{m1} decide the inlet angle.

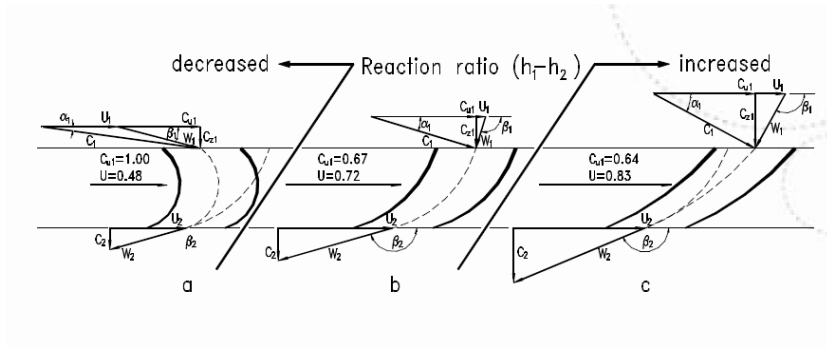Figure 3.1: Different reaction degrees [Bre03]

3.1.2   Pool pair number

The number of pool pairs in the generator, together with the grid frequency, will determine the rotational speed of the runner. In order to create a grid frequency of 50 H_z the rotor in the generator has to pass 50 pool pairs in the stator per second. The following equation will determine the runner's revolutions per minute.

$$n = \frac{60 \cdot f_{grid}}{Z} \qquad [\text{rpm}] \qquad (3.4)$$

Here Z is the number of pool pairs, and n is the rotational speed. Nepal has a grid frequency of 50 H_z. Since we now know both the angular velocity at the runner inlet and the rotational speed, we can easily calculate the inlet diameter.

$$D_1 = \frac{60 \cdot U_1}{\pi \cdot n} \qquad [\text{m}] \qquad (3.5)$$
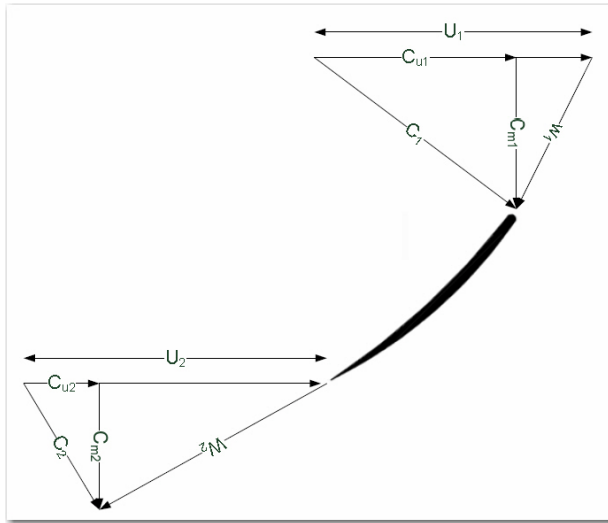
3.1.3 Outlet Angle

Figure 3.2: Inlet and outlet velocity diagram [Fra08]

From figure 3.2, and the design criteria: no swirl in the draft tube, two expressions for C_{m2} can be derived.

$$C_{m2} = U_2 \tan \beta_2 \qquad [\text{m/s}] \qquad (3.6)$$

$$C_{m2} = \frac{Q}{A} = \frac{4 \cdot Q}{\pi \cdot D_2^2} \qquad [\text{m/s}] \qquad (3.7)$$

U_2 can be desribed as

$$U_2 = \frac{D_2 \cdot \pi \cdot n}{60} \qquad [\text{m/s}] \qquad (3.8)$$

If combining equation 3.6 3.7 and 3.8, a expression for D_2 can be derived.

$$D_2 = \sqrt[3]{\frac{60 \cdot 4 \cdot Q}{\pi^2 \cdot n \cdot \tan \beta_2}} \qquad [\text{m}] \qquad (3.9)$$

After calculating D_2, equation 3.8 can be used to find U_2. Then C_{m2} can be found through equation 3.6. In order to avoid backflow in the runner, a design rule of thumb is that C_{m2} is 10% larger than C_{m1}. This will provide acceleration through the runner.

$$C_{m1} = \frac{C_{m2}}{1.1} \qquad [\text{m/s}] \qquad (3.10)$$

The last main dimension to calculate is the height at the inlet.

$$B = \frac{1.1 \cdot D_2^2}{4 \cdot D_1} \qquad [\text{m}] \qquad (3.11)$$

3.2 Runner

3.2.1 Axial view

In order to design the runner geometry, an axial view has to be constructed. There are many ways to do this, but in this thesis, the continuity approach starting at the shroud has been used. The start and stop points for the streamline at the ring is found through the main dimension equations. In between, the ring coordinates is a matter of choice. In this thesis a segment of an ellipsis has been used to construct the ring. In order to avoid the streamlines making an upwards curvature, the segment need to be less than

one quarter. This means that the water velocity already has a downward component at the ring starting point. Since the inlet height of the runner is known from the main dimension equations, you already know the starting point for the other streamlines. Then the algorithm is to fill in the remaining points through continuity considerations. A detailed description of those equations can be found in[Elt09]
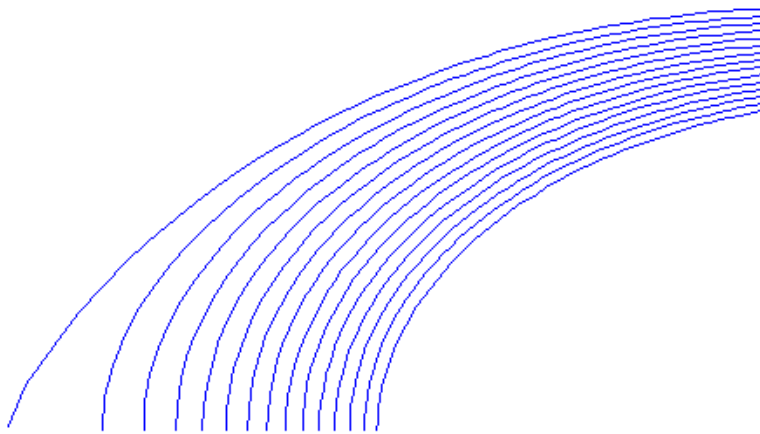
Figure 3.3: Axial view of the runner

3.2.2 UC_u

When the water travel trough the runner, it is loosing much of its energy. This is the very meaning with the runner, converting the waters energy into mechanical energy the generator can utilize to create electricity. The energy converting happens because the water acts with a force on the runner blade. The force equals the change in velocity times the mass flow.

$$F = \dot{m} \cdot (C_{u1} - C_{u2}) \qquad [\text{N}] \qquad (3.12)$$

Since this force is acting on a rotating runner some distance from the

shaft center, the torque and effect become:

$$T = \dot{m} \cdot (C_{u1} \cdot r_1 - C_{u2} \cdot r_2) \qquad \text{[Nm]} \qquad (3.13)$$

$$P = \omega \cdot T = \dot{m} \cdot \left(C_{u1} \cdot r_1 \cdot \frac{U_1}{r_1} - C_{u2} \cdot r_2 \cdot \frac{U_2}{r_2} \right) \qquad \text{[W]} \qquad (3.14)$$

$$P = \dot{m} \cdot (C_{u1} \cdot U_1 - C_{u2} \cdot U_2) \qquad \text{[W]} \qquad (3.15)$$

As seen in equation 3.15, the power output from the runner is proportional to the change in $U \cdot C_u$.

3.2.3   Energy distribution

In order to find the radial view of the runner, the energy distribution through the runner has to be decided. The energy conversion from the water to the shaft will be the minus derivative to this distribution. That is the change in radial kinetic energy. The angle of the blade can now be calculated from the following equations.

$$C_u = \frac{U C_u}{U} \qquad \text{[m/s]} \qquad (3.16)$$

$$\beta = \arctan \frac{C_m}{U - C_u} \qquad \text{[rad]} \qquad (3.17)$$

3.2.4   G-H view

Since we now know both the length of the streamlines in the axial view and the blade angle through the runner, a view of the runner blade from above can be constructed. This is called the G-H view. The G stands for the length of the streamline in the axial plane, H for the streamline length in the radial plane. To calculate ΔH, equation 3.18 is used.

$$\Delta H = \frac{\Delta G}{\tan \beta} \qquad \text{[m]} \qquad (3.18)$$
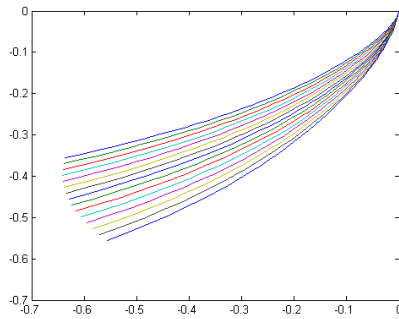
Figure 3.4: an example of a H-G view

Then it is easy to find the radial view of the runner. Simply use the equation 3.19 to find the theta angle. See figure 3.5 in order to find the notation used.

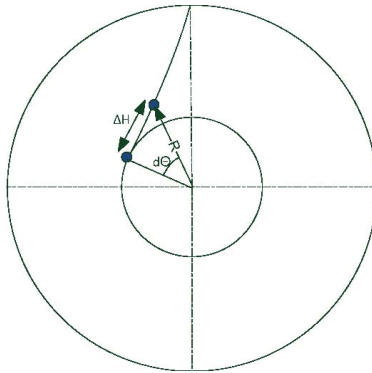$$d\theta = \frac{\Delta H}{R} \qquad [\text{rad}] \qquad\qquad (3.19)$$

Figure 3.5: Radial view [Elt09]

3.3   Guide vanes

Here follows the algorithm used in this thesis to design the guide vanes.

1. Calculate the outlet diameter of the guide vanes. This diameter should be around five percent larger than the runner's inlet diameter.

2. Calculate both components of the outlet velocity from the guide vanes, the velocity angel and the outlet total velocity. C_{mgvo} is found through the conservation of mass law 3.20. C_{ugvo} is found through the free vortex assumption 3.21.

$$C_{mgvo} = \frac{Q}{\pi \cdot D_{gvo} \cdot B_{gvo}} \qquad [\text{m/s}] \qquad (3.20)$$

$$C_{ugvo} = \frac{C_{u1} \cdot D_1}{D_{gvo}} \qquad [\text{m/s}] \qquad (3.21)$$

$$\tan \alpha_0 = \frac{C_{mgvo}}{C_{ugvo}} \qquad [\text{rad}] \qquad (3.22)$$

3. Calculate the initial axis diameter of the guide vanes. This can be done with Brekkes equation.

$$D_{axf} = D_1 \cdot (0,29 \cdot \Omega + 1,07) \qquad [\text{m}] \qquad (3.23)$$

Where Ω is the speed number.

4. Calculate the length of the guide vanes.
   Because the guide vanes are supposed to be able to stop the water flow if necessary, a minimum length can be calculated from the axis diameter and the number of vanes. Since we don't want the vanes to manage to rotate a full circle, it is necessary to add an overlap factor to the equation. Normally about 10-15 percent is chosen. The equation then will be as follows.

$$L_{gv} = \frac{\pi \cdot D_{axf} \cdot k_{cf}}{N_{gv}} \qquad [\text{m}] \qquad (3.24)$$

5. Calculate the guide vanes outlet diameter.
Then both the outlet and guide vane axis diameter is known, the inlet
diameter can be found through the cosine theorem.

$$D_{gvi} = 2 \cdot \sqrt{L_{gv}^2 + \frac{D_{gvo}^2}{4} - 2 \cdot L_{gv} \cdot \frac{D_{gvo}}{2} \cdot \cos\left(\frac{\pi}{2} + \alpha_0\right)} \qquad [\text{m}]$$
$$(3.25)$$

6. Based on the calculated inlet diameter, both the guide vane diameter
and coverage factor has to be recalculated. Normal practice is that
the guide vane axis is located around 2/3 of the guide vane length
upstream of the guide vane outlet.

7. Finally it is necessary to choose an airfoil. A nice place to start
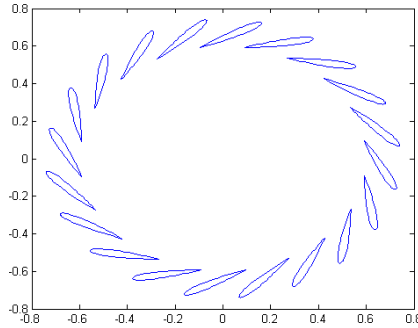searching can be through the different NACA profiles.

Figure 3.6: Guide Vanes

3.4   Stay vanes

The reason for the stay vanes to exist, is to keep the spiral casing together. In other words, the stay vanes absorb the force from the water acting on the steel. Because of high heads and the effect of water hammer, this force can be enormous. The following equation is used to calculate the maximum pressure the stay vanes have to resist.

$$P_{max} = P_{head} + P_{waterhammer} \qquad \text{[Pa]} \qquad (3.26)$$

The maximum force is then:

$$F_{max} = P_{max} \cdot A_{annulus} \qquad \text{[N]} \qquad (3.27)$$

To calculate the length of the stay vanes, both the number of stay vanes and the average thickness have to be decided. Then equation 3.28 is used.

$$L_{sv} = \frac{F_{max}}{\rho_{steel} \cdot t_{sv} \cdot N_{sv}} \qquad \text{[m]} \qquad (3.28)$$

The curvature of the stay vane is calculated through the free vortex assumption and the conservation of mass law. The stay vane outlet diameter is normally set to be 2 percent larger than the guide vane inlet diameter.
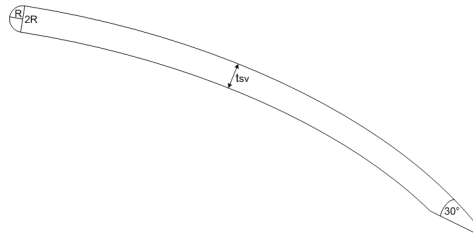

Figure 3.7: Example of a stay vane

3.5   Spiral Casing

The main task of the spiral casing is to deliver equal amount of water throughout the runner's perimeter. This is obtained because the cross section of the spiral casing gets smaller as water exits to the runner. From the previous calculations the vanes inlet diameter and height are known.

To stop a secondary flow pattern in the casing, it is normal practice to let the stay vanes overlap the casing with a factor $k_2 \cdot B$. For high head Francis turbines it is usual to set $k_2 = 0,1$ [Bre03].
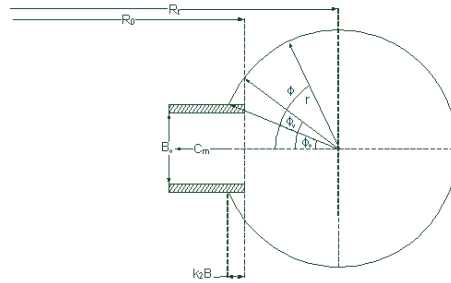

Figure 3.8: View of the Spiral Casing [Fra08]

To find the r and R_t the following equations are used in an iteration process for each section of the spiral casing. This is taken from [Bre03].

$$R_t = R_0 + r \cdot \cos \phi_0 - k_2 \cdot B \qquad [\text{m}] \qquad (3.29)$$

$$Q = 2r^2 C_t \int_{\phi_y}^{\pi} \frac{\sin^2 \phi}{R_t - r \cdot \cos \phi} d\phi \qquad [m^3/s] \qquad (3.30)$$

The iteration algorithm is stated under.

• Set a start value for r.

- Calculate ϕ_o and ϕ_y through geometric calculations. See figure 3.8.

- Solve the integral in equation 3.30.

- Calculate a new r through equation 3.30.

This iteration process is repeated until r has converged within an acceptable error. An example of a spiral casing, generated by the matlab-code following this thesis, is shown in figure 3.9.
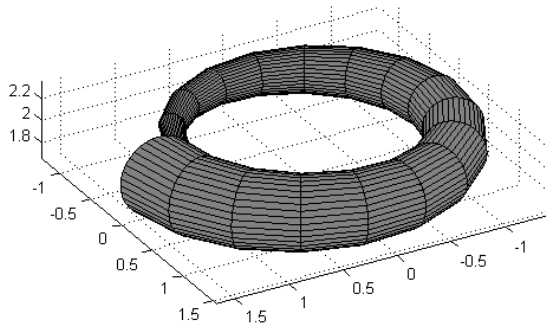
Figure 3.9: Spiral Casing

Chapter 4

Velocity Theory for Francis Turbines
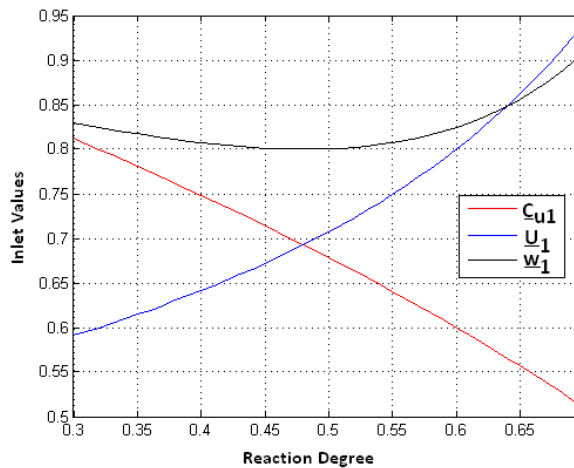
4.1   Optimal reaction degree

Figure 4.1: Inlet values

As seen from figure 4.1 The reaction degree will determine the relative velocity at the inlet. The lowest value for the inlet relative velocity is obtained when the radial component of the velocity is zero. This means that the inlet angle beta equals 90 degrees. In order to find this reaction degree value mathematically, we state that U_1 and C_{u1} are equal. From equation 3.2 and 3.3 we then derive the following expression:

$$R = \frac{\eta_h}{2} \qquad [\text{-}] \qquad (4.1)$$

4.2 Optimal outlet diameter

In this section, the outlet diameter which gives the lowest outlet relative velocity will be derived. The outlet relative velocity has two components, U_2 and C_{m2}, see equation 3.7 and 3.8. When changing the outlet angle β_2, those two components also change. This can easily be seen from figure 3.2. If increasing β_2, also C_{m2} increases. Then, because of the conservation of mass law, the outlet diameter will become smaller, which reduces the U_2 component. The idea is that since a change in the outlet conditions always increase one component of the relative velocity and reduce the other one, an optimum point can be found where the relative velocity has its lowest value possible. To find this point, the outlet relative velocity equations derivative with respect to the outlet diameter is derived and put equal to zero. Secondly, equation 3.9 is used to find what the outlet angle of the corresponding outlet diameter.

$$w_2 = \sqrt{U_2^2 + C_{m2}^2} = \sqrt{\frac{16 \cdot Q^2}{\pi^2} \cdot \frac{1}{D_2^4} + \frac{\pi^2 \cdot n^2}{3600} \cdot D_2^2} \qquad [\text{m/s}] \qquad (4.2)$$

$$\frac{dw_2}{dD_2} = \frac{1}{2 \cdot \sqrt{\frac{16 \cdot Q^2}{\pi^2} \cdot \frac{1}{D_2^4} + \frac{\pi^2 \cdot n^2}{3600} \cdot D_2^2}} \cdot \left(2 \cdot D_2 \frac{\pi^2 \cdot n^2}{3600} - \frac{4 \cdot 16 \cdot Q^2}{\pi^2 \cdot D_2^5} \right) \qquad [m/s^2]$$

$$(4.3)$$

When put equal to zero, the expression for optimal outlet diameter is found.

$$D_2 = \sqrt[6]{\frac{115200 \cdot Q^2}{\pi^4 \cdot n^2}} \qquad [\text{m}] \qquad (4.4)$$

The corresponding outlet angle is found by putting equation 4.4 into equation 3.9

$$\beta_2 = \arctan \frac{1}{\sqrt{2}} \qquad [\text{rad}] \qquad (4.5)$$

This means that the lowest relative outlet velocity, and hereby the erosion, occur when equation 4.5 is satisfied. This finding is valid for every power plant. The optimal outlet angle will be around 35 degrees, as seen in figure 4.2.
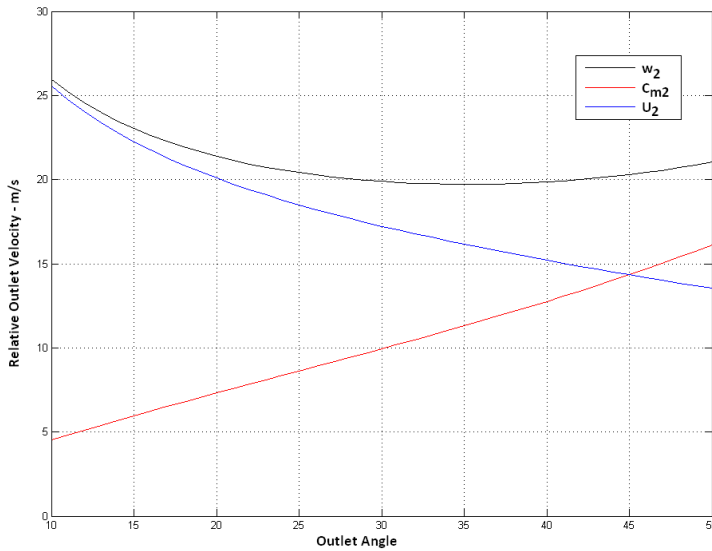

Figure 4.2: Outlet relative velocity with its two components

From figure 4.3 we see how the outlet relative velocity changes for different pole pair numbers and outlet diameters.
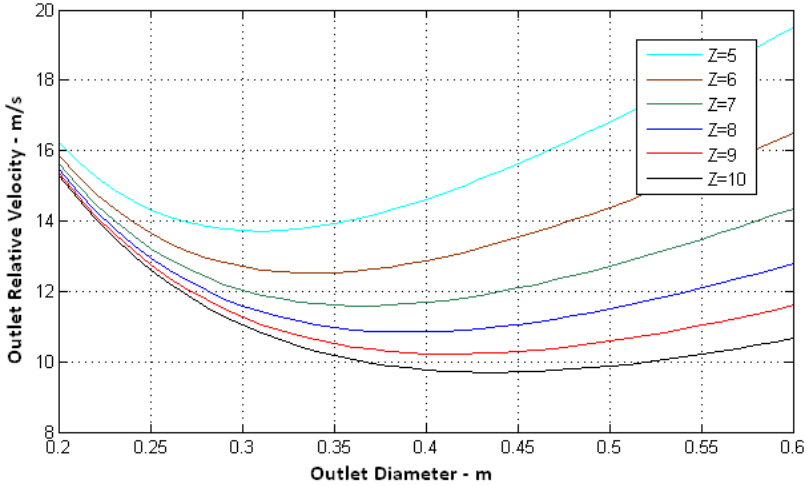

Figure 4.3: Relative outlet velocity for Jhimruk power plant. The flow rate equals 7 m^3/s

in this figure.

Since the outlet angle also changes the relative inlet velocity, it is useful to derivative the inlet relative velocity with respect to the outlet diameter. This gives us a deeper understanding of the change.

$$w_1 = \frac{240 \cdot Q}{60 \cdot 1, 1 \cdot \pi \cdot D_2^2} \qquad [\text{rad}] \qquad (4.6)$$

$$\frac{dw_1}{dD_2} = -\frac{8 \cdot Q}{1, 1 \cdot \pi \cdot D_2^3} \qquad [\text{rad}] \qquad (4.7)$$

This expression will never equal zero, which yields that the graph has neither any top nor any bottom points.

4.3 Change of the relative velocity through the runner

In order to describe the change of relative velocity through the runner, it is necessary to understand how its two components change.

- C_m has a linear increase through the runner. This acceleration is decided when designing the axial view of the runner.

- The radial component consists of two components. The rotational speed of the runner which is proportional to the radius, and is therefore almost linear, because the runner's axial view has the form of an ellipsis, and the change of radius per length step is therefore not constant. We are free to choose the C_u through the UCu distribution. However, C_{u2} should always be zero when in operation at the best point, in order to get the highest efficiency possible.

Because of this, the radial component is strongly increased at the end of the runner, as shown in figure 4.4. The radial component in the example of figure 4.4 is zero at the runner inlet because the reaction degree has been set equal to the hydraulic efficiency half.
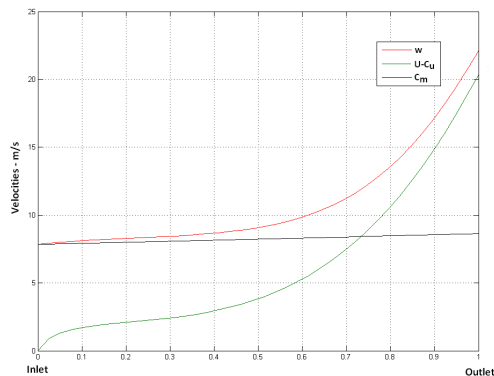

Figure 4.4: example of relative velocity through runner

4.4 Relative velocity change due to UCu distribution

In this section, we will study how the UC_u distribution will change the relative velocity through the runner. When the main dimensions of the turbine have been decided, both the angular velocity of the runner and Cm through the runner is given by respectively equation 4.8 and 4.9.

$$U = \frac{2\pi \cdot n}{60} \cdot r \qquad \text{[m/s]} \qquad (4.8)$$

$$C_m = C_{m1} + C_{m1} \cdot 0.1 \cdot relativesection \qquad \text{[m/s]} \qquad (4.9)$$

The relative velocity though the runner is given by:

$$w = \sqrt{(U - C_u)^2 + C_m^2} \qquad \text{[m/s]} \qquad (4.10)$$

When the main dimensions are calculated, our only possibility to change the relative velocity through the runner is to change the waters radial absolute velocity in the runner. This is done by changing the UCu distribution.

$$C_u = \frac{U \cdot C_u}{U} \qquad \text{[m/s]} \qquad (4.11)$$

When trying to solve the sand erosion problem in Francis turbines, our goal should be to reduce the radial component of the relative velocity as much as possible. To achieve this, the following equation should be satisfied. This component is tried illustrated as the marked area in figure.

$$C_u - U = 0 \qquad \text{[m/s]} \qquad (4.12)$$

This means that the rotational speed of the runner equals the radial component of the waters velocity. Figure 4.5 tries to illustrate the radial component of the relative velocity when the UCu distribution is linear.
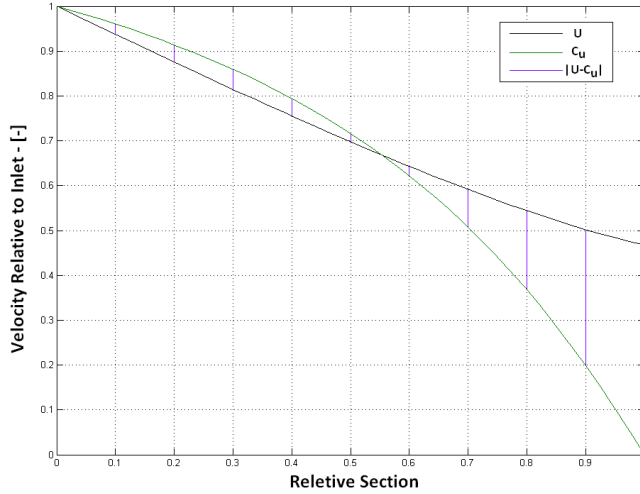
Figure 4.5: Design with a linear UCu distribution

4.5 Friction theory

One of the sources of energy loss through the turbine is friction between
the water and the different steel surfaces. These surfaces mainly consist
of the runner, guide vanes and the stay vanes. Since this thesis consist
of testing many different turbine designs, it is of interest to see how the
friction loss from the turbine changes with the different designs. To do so,
the Darcy-Weisbach equation 4.13 has been used[Whi08].

$$H_f = f \cdot \frac{L}{D_h} \cdot \frac{V^2}{2g} \qquad \text{[m]} \qquad (4.13)$$

Where
h_f is the head loss due to friction.
L is the length of the surface.
D is the hydraulic diameter of the surface.

V is the relative velocity between water and surface.
f is a dimensionless friction coefficient. This can be found through the Moody diagram.

The hydraulic diameter is defined as:

$$D_h = \frac{4A}{P} \qquad [\text{m}] \tag{4.14}$$

Where A is the cross section area and P is the wetted perimeter of the area defined as A.

Chapter 5

Ideas to Reduce Sediment Erosion

5.1 Change of different runner parameters

The idea to reduce the sediment erosion in the runner is to change different parameters from the values normally used today. The different parameters which are thought to have an impact on the runner velocity, and hereby the erosion, is: reaction degree, outlet angle, number of pole pairs and the UCu distribution. The results of changing these parameters are shown in the result chapter.
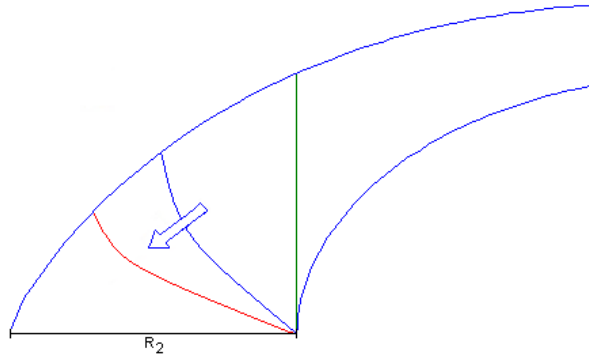
5.2   Shape off Blade Trailing Edge

Figure 5.1: Axial view of a runner

Since the water doesn't have any rotation at the runner outlet, the relative outlet velocity in the radial direction is given by the following equation:

$$W_{uoutlet} = r_{outlet} \cdot \omega \qquad [\text{m/s}] \qquad (5.1)$$

In other words, the velocity is proportional to the radius. This means that we, is possible, want to reduce the outlet radius. An optimal value for the outlet diameter, and thereby also the radius, was derived in the chapter, Velocity theory for Francis turbines. However, this value refers only to the radius at the bottom of the runner,R_2, see figure 5.1. Normal practice of turbine design over the years has been to cut the runner's trailing edge, because the extra steel it would represent is thought not to be necessary. However, we now need to redo this thinking, since this cutting increases the radius and thereby the erosion. The criteria when deciding where to cut the runner's trailing edge should be to cut no more than necessary. To illustrate my point, and take it to the extreme, consider the green line to be the outlet of the runner. This means that we have the relative outlet velocity that is normally found only at the bottom point at the outlet over

the whole outlet. As will be shown in some figures to come, this is where the velocity is biggest. In the other end, not cutting the runner gives the same relative velocity at the top outlet point as at the inlet. This phenomenon is captured in figure 5.2
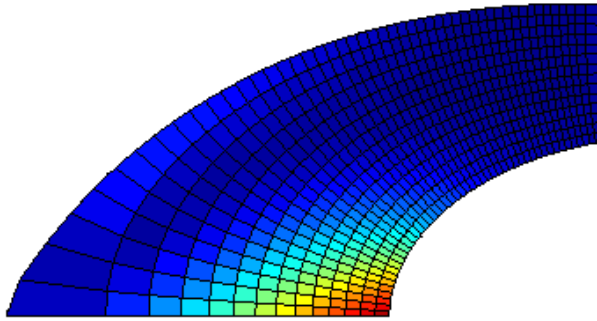

Figure 5.2: Axial view of a runner that has not been cut
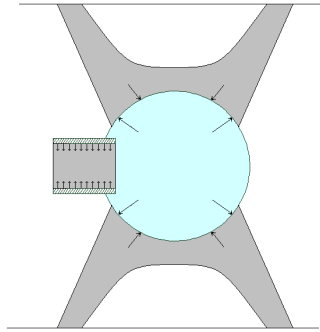
5.3 remove stay vanes

Figure 5.3: Spiral casing with both inside and outside stay vanes

Since the stay vanes are exposed to severe erosion problems due to the high velocity of the water, an idea is to simply remove them from the turbine inside, putting them on the outside instead. Their function is to hold the spiral casing together, in other words absorb the forces from the water acting on the casing. As shown in figure 5.3 this can be done both from the inside and outside of the spiral casing. To design the exact geometry of the new type of stay vanes is considered to be outside of the scope of this thesis since we already know that it is possible to absorb the forces in that way. One example has been drawn in figure 5.4. Note that this drawing only shows the bottom side of the stay vanes. The same vanes also need to be placed on top of the spiral casing.
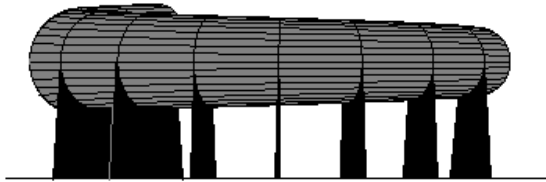
Figure 5.4: Spiral casing with outside stay vanes

5.4   remove guide vanes

Because of high water velocity through the guide vanes, these vanes are
affected by sand erosion. As seen at the picture 5.6, the most affected part
is the vanes top and bottom side. This is due to the fact that some amount
of water is flowing through the small gap between the guide vanes and its
cover. Also the corresponding top and bottom cover is highly affected, see
picture 5.5.

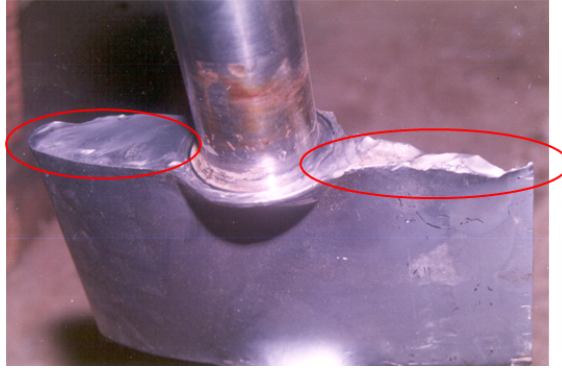Figure 5.5: Eroded guide vane cover[Dah]

Figure 5.6: Eroded guide vane[Dah]

In this section, we will look into the possibilities to remove all trouble of guide vane erosion by removing the guide vanes itself. The first question to ask is: why are they there in the first place? And secondly, can other components do the job the guide vanes are supposed to do. If they can, we might be able to remove them and the problems they cause

So, the guide vanes are supposed to do three things. The first is to deliver a correct inlet flow of water to the runner. Secondly they act as a safety valve in case of failure of the spherical valve. This is because a spherical valve, commonly in use in today's power plants, cannot open when there only is high pressure on one side of the valve, see figure 5.7. Thirdly, for high head turbines, they act as a valve when trying to start the turbine after time without running.
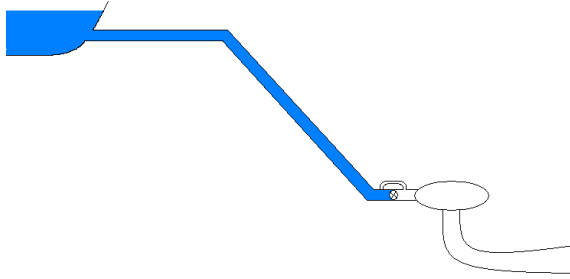
Figure 5.7: Eroded guide vane

When one should open the spherical valve after a shutdown of the power plant, water is bypassed over the spherical valve, and the pressure downstream the valve is increasing until it equals the pressure upstream, see figure 5.8. By doing so, the valve can open. This is the way the valve is opened in today's power plants.
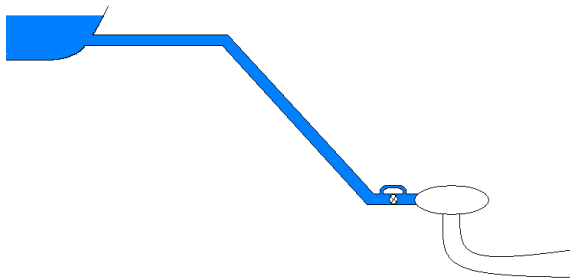

Figure 5.8: Eroded guide vane

If the guide vanes shall be removed, another way of opening the spherical valve has to be applied. One such method is tried illustrated in figure 5.9. The only new component is a valve in the low pressure section of the pipe line. Because of the low pressure, this valve does not need to be as expensive or advanced as the spherical valve. The idea is to equalize the pressure

upstream of the spherical valve, to the atmospheric pressure downstream. This is done by simply bypassing the water over the runner 5.9. This method also needs an air inlet into the pipe system, to avoid under pressure in the pipeline. The safety of the system is preserved since two independent valves can stop the water flow in case of emergency. However, this method has one serious disadvantage. That is at the start up of the turbine, where the water is hitting the runner with an high velocity.
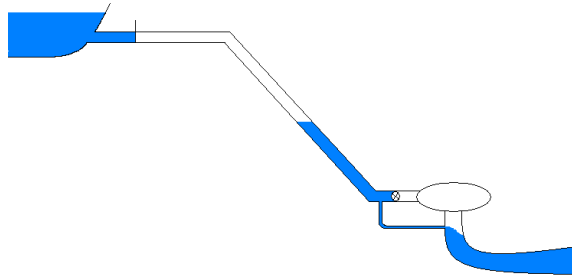

Figure 5.9: Eroded guide vane

Another solution can be to redesign the spherical valve so it can open despite a huge pressure difference between its two sides.

Chapter 6

Results

Installed effect	12 MW
Head	201,5 m
Total flow	7 m^3/s
Flow each turbine	2,35 m^3/s
Z	3
R	0.52
β_2	18 degrees
Units	3

Table 6.1: Jhimruk Power Plant[Yad04]

In order to find the best design with regard to sand erosion, two sand erosion parameters have been defined. The first parameter is the thickness of erosion per unit time the sand will erode of the turbine, see equation 2.2. The second is something denoted the erosion rate in this thesis. The parameter is defined in equation 6.1:

$$Erosionrate = \frac{W}{Area} \qquad [1/m] \qquad (6.1)$$
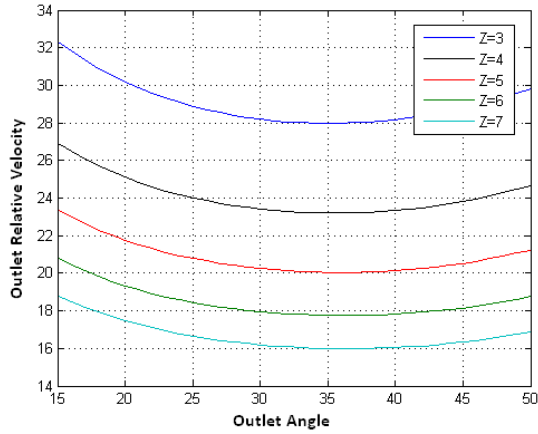
6.1 Relative inlet and outlet velocity

Figure 6.1: Relative outlet velocity

Figure 6.1 shows the outlet relative velocity as a function of pole pair number and outlet angle. From this figure we clearly recognize the optimal outlet velocity described in the theory section.
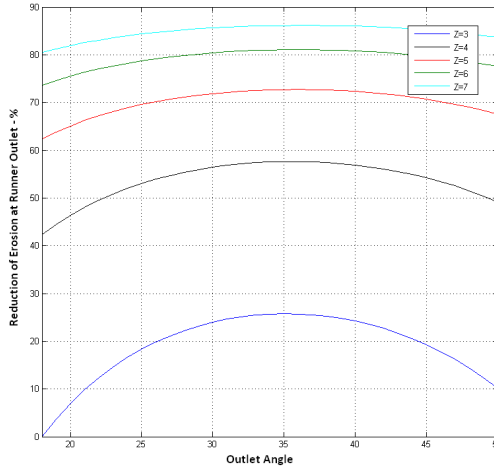
Figure 6.2: Sand erosion reduction at Jhimruk's runner outlet

Figure 6.2 shows the reduction of the outlet erosion in percent compared to today's runner.
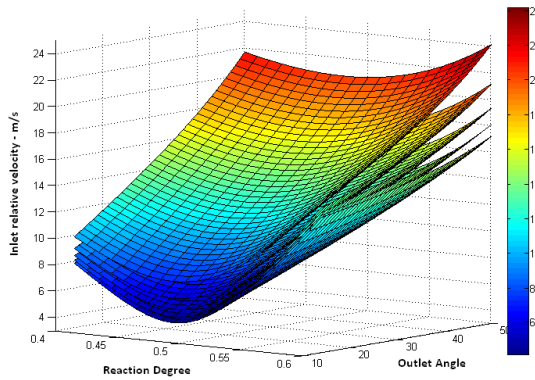

Figure 6.3: Relative inlet velocity

Figure 6.3 shows how the relative velocity at the inlet change when changing the reaction degree, pole pair number and outlet angle. Each pole pair number is represented by one surface area. At the lowest surface the pole pair number is three. The following surfaces represent a pole pair number from four to seven.
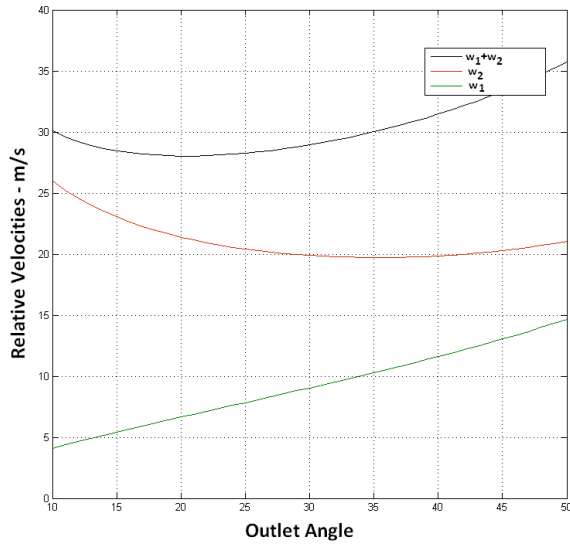

Figure 6.4: Relative inlet and outlet velocity

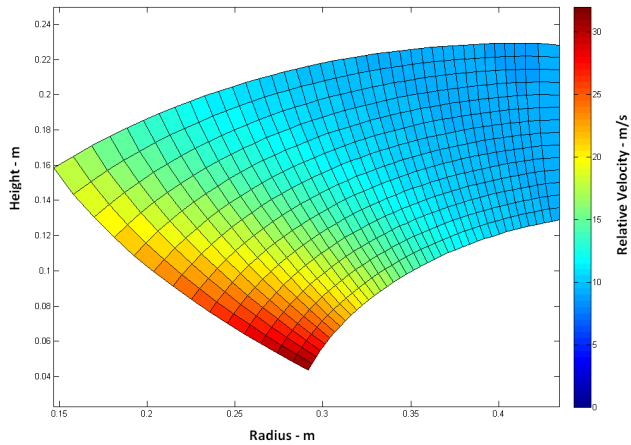## 6.2 Changing the reaction degree, outlet angle and pole pair number

Figure 6.5: Todays Jhimruk runner

Figure 6.6: Damage of runner outlet[Dah]

This is the today's runner at Jhimruk power plant. As seen from figure 6.5, the relative velocity is highest at the lowest outlet point. Here the relative velocity is around 30 m/s. That is quite a difference from the inlet, where the relative velocity is only around 7 m/s. These results explains why the power plant has severe erosion problems at the lowest outlet point, see picture 6.6. The UCu distribution for today's runner is set to be linear.
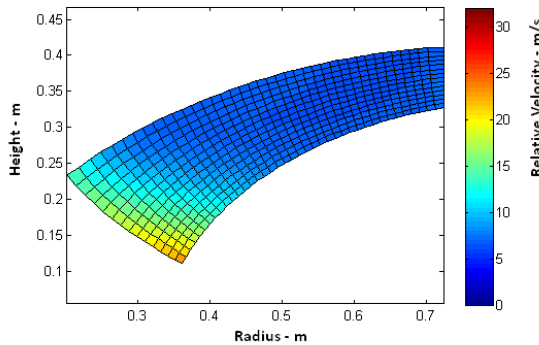
Figure 6.7: R=0.52, β_2=18, Z=5

The first step in showing how the parameters chosen in this thesis is changing the runner and its relative velocity, is to change the number of pole pairs in the generator. The number is increased from three to five, and by doing so, reducing the angular speed from 1000 to 600 rpm. When comparing figure 6.5 and 6.7, we see that this change is very powerful in order to reduce the erosion. The highest relative velocity is now only around 22 m/s. Changing the pole pair number will also make the runner blade longer and thinner.
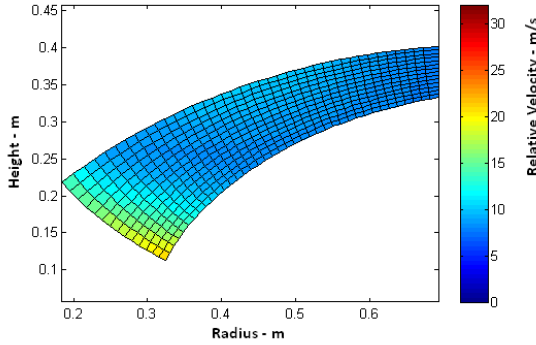
Figure 6.8: R=0.48, β_2=25, Z=5

The next step is to change both the reaction degree and the outlet angle. From the theory "optimal reaction degree", the reaction degree is calculated to be 0,48. The outlet angle is chosen to be 25 degrees. As seen in figure 6.8, the inlet relative velocity has been increased a little, but this change is barely noticeable. At the outlet, changing the outlet angle has clearly reduced the relative velocity.

6.3   Changing the UCu distribution

In this section we look into how the UCu distribution is changing the relative velocity in the runner. The other parameters are the same as in figure 6.8 Two of the distributions that was tested are shown in figure 6.9 as the black and green graph. The red graph is the linear distribution that has been used in the results so far. At the end an optimal distribution is tested. Together, these distributions will be presented in the next three subsections.

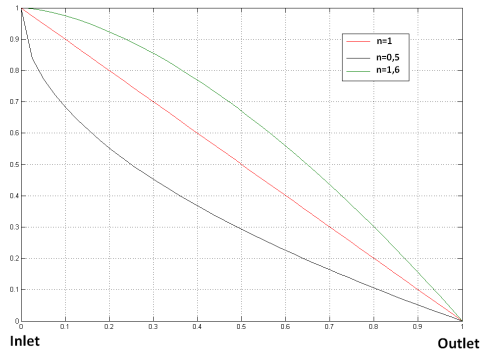Figure 6.9: The different UCu distributions tested

The mathematical expression of all the distributions tested, except the optimal one, is on the following form.

$$UC_u = 1 - x^n \qquad \text{for} \quad x \in 0 - 1 \qquad [\text{-}]$$

n has been changed from 0,5 to 1,6.

The erosion rate for the different distributions is shown in figure 6.10.
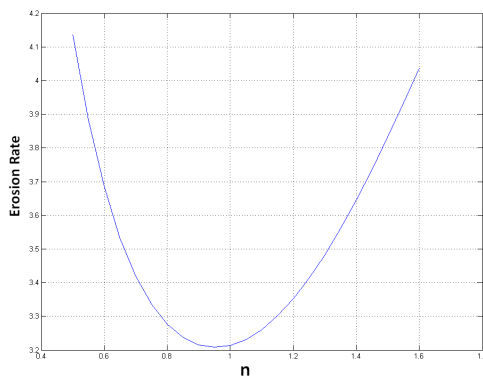
Figure 6.10: Erosion Rate for different n in equation 6.3

6.3.1   The black distribution

Figure 6.11: New design with the black distribution from figure 6.9

Figure 6.12: the radial velocities from inlet to outlet

At this UCu distribution, most of the energy in the water is transferred into shaft energy at the outer part of the runner. the radial component of the relative velocity vector is quite large all the way through the runner,

as shown in figure 6.12. This gives the runner a large relative velocity in nearly all sections, as shown in figure 6.11.

6.3.2 The green distribution

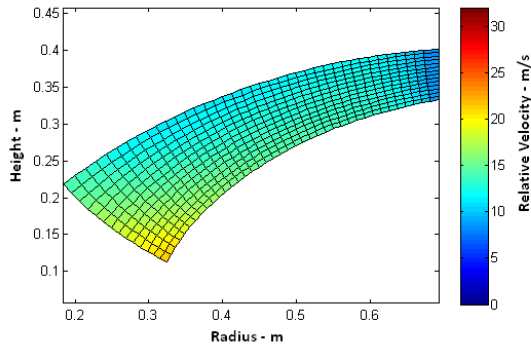
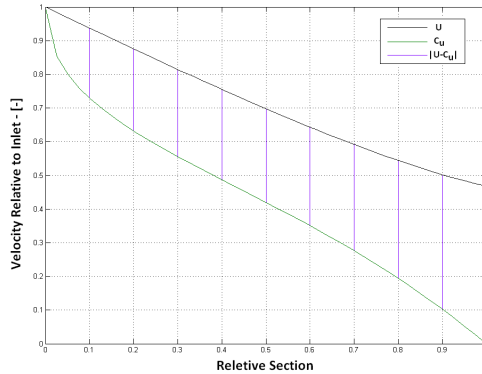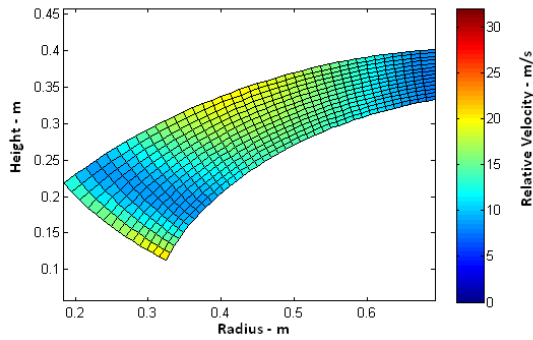Figure 6.13: New design with the green distribution from figure 6.9
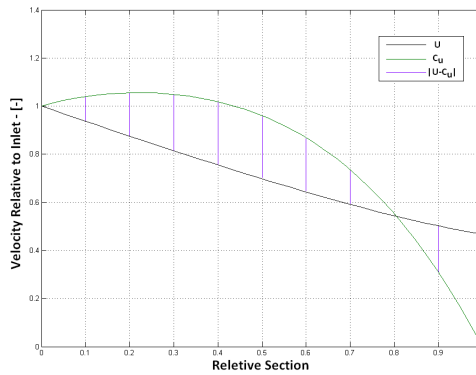
Figure 6.14: the radial velocities from inlet to outlet

At this UCu distribution, most of the energy in the water is transferred into shaft energy at the inner part of the runner. An interesting thing has occurred, the radial component of the relative velocity is at first positive seen from the inlet, then becomes zero before turning negative, see figure 6.14. In figure 6.13, the point where the radial component equals zero can easily be spotted.

6.3.3 The optimal UCu distribution

The optimal UCu distribution occurs when equation 4.12 is satisfied for as long as possible. Because of the no swirl design criteria, this cannot be the case at the end of the runner.
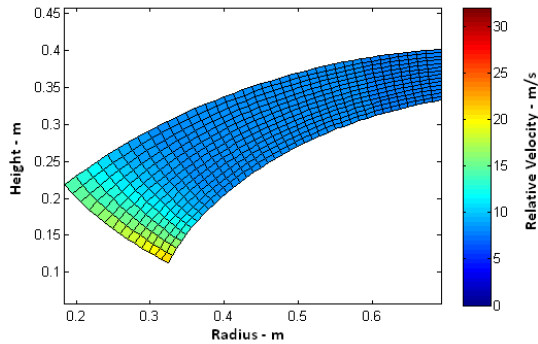
Figure 6.15: Optimal $U \cdot C_u$ distribution
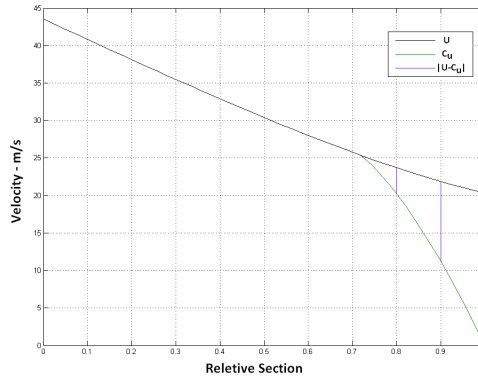
Figure 6.16: the radial velocities from inlet to outlet

In figure 6.15 and 6.15, the optimal UCu distribution approach has been applied.

As seen from these graphs, by changing the UCu distribution, it is possible to greatly change the radial component of the relative velocity, marked as the purple lines in figure 6.12, 6.14 and 6.16, through the runner.

6.4 Erosion Rate

Here follow the erosion rates of runners with different reaction degrees, outlet angles, pole pair numbers and UCu distributions. Each figure corresponds to one UCu distribution. Each surface area in a figure corresponds to one number of pole pairs. The two last parameters can be found in two of the axis, and the height corresponds to the erosion rate. The figures draw the surface area to the pole pair number from three to seven. The top surface is that of three pole pairs.

6.4.1 With a linear UCu distribution
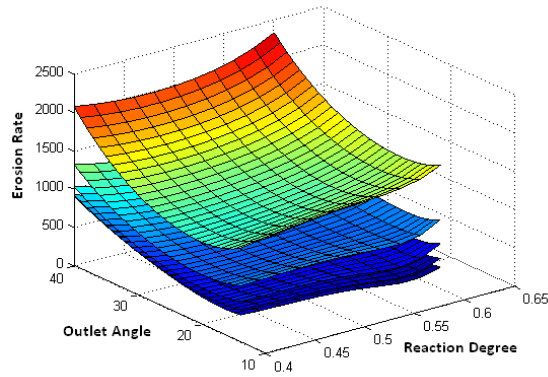
Figure 6.17: Erosion Rate change with $U \cdot C_u$

6.4.2 With n=0,5 in the UCu distribution
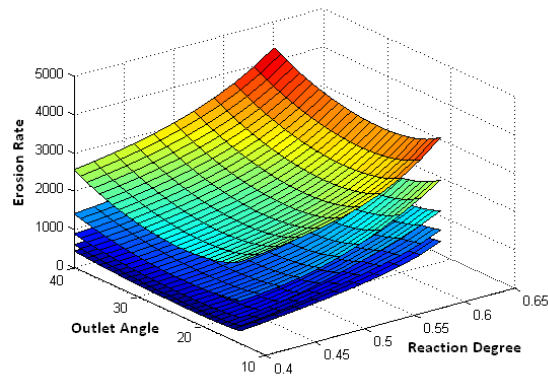
Figure 6.18: Erosion Rate change with $U \cdot C_u$

6.4.3   With optimal UCu distribution
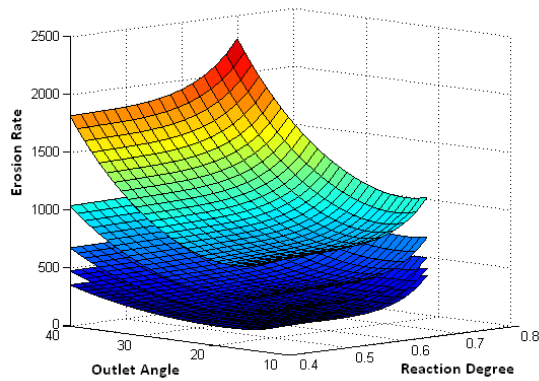
Figure 6.19: Erosion Rate change with $U \cdot C_u$

6.4.4   Erosion Rate vs Blade Area vs Eroded Steel
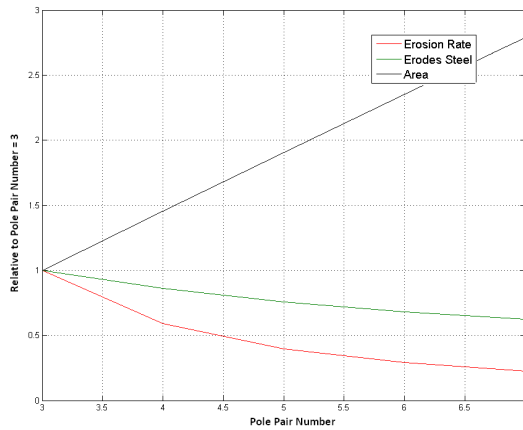
Figure 6.20: changing pole pair number

Figure 6.20 shows how the runner area, the thickness of erosion from equation 2.2 and the erosion rate change with respect to the pole pair number.
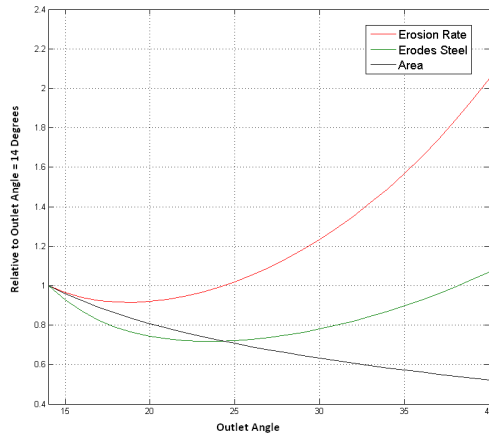
Figure 6.21: changing outlet angle

Figure 6.21 shows how the runner area, the thickness of erosion from 2.2 and the erosion rate change with respect to the outlet angle.

6.5   Erosion in Guide Vanes and Stay Vanes
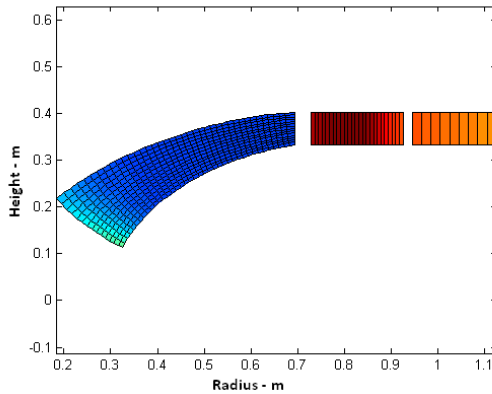
Figure 6.22: Velocity through the whole turbine

Figure 6.22 shows the absolute velocity in the guide and stay vanes and the relative velocity in the runner cascade.

6.5.1   Guide Vanes

The two following figures that follow show the erosion in the guide or stay vane cascade for different values for the reaction degree, outlet angle and pole pair number. Each surface area represents one pole pair number. The top area is for three pole pairs. The bottom surface is for five.
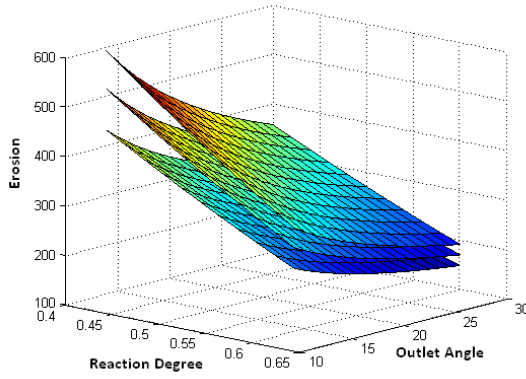
Figure 6.23: Erosion in Guide Vanes at different parameters

6.5.2   Stay Vanes
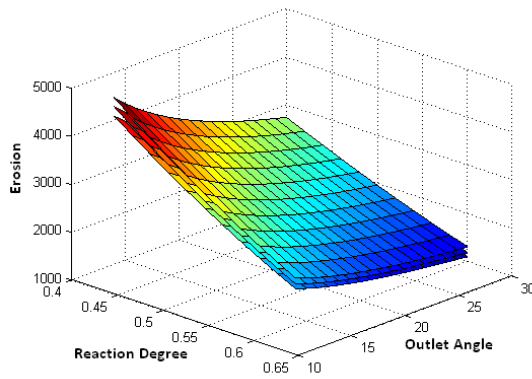
Figure 6.24: Erosion in Guide Vanes at different parameters

6.6 Final Jhimruk Runner Geometry

6.6.1 Without Guide Vanes
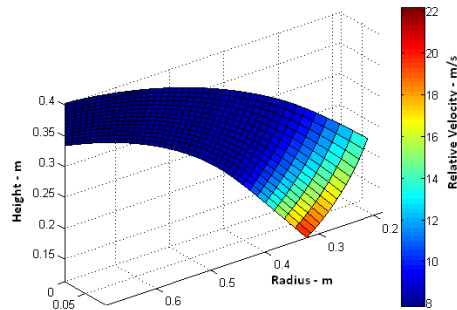
Figure 6.25: Runner Geometry with reaction degree equal to 0,48

6.6.2 With Guide Vanes
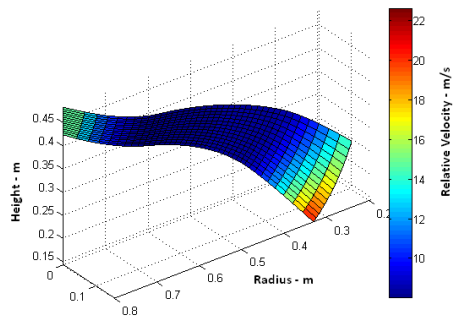
Figure 6.26: Runner Geometry with reaction degree equal to 0,6

6.7 CFD-Analysis

A CFD analysis has been conducted at the runner's best point. The results are shown in the figures to follow. The different setup used will also briefly be described.

Quartz is one of the hardest sediments present in most power plants exposed to sediment erosion, rated as number seven on Moh's hardness scale[Tha10]. This combined with its high concentration at Jhimruk power plant made it natural to choose the constant values for quartz particles and steel wall following Tabakoff's equation. These values can be found in[fun09].

The mesh for the CFD analysis was made in Ansys Turbogrid. It has a total of 933464 nodes and 885280 elements. What Turbogrid calls an o-grid has been included around the blade in the boundary layer. In other words, the mesh has a much higher element density in the boundary layer that surrounds the blade. This was done because the flow has much higher gradients near a wall. The mesh has also been divided into two different domains, one for the runner blade and one for the draft tube.

There are four different boundary conditions in this analysis. The hub, blade and shroud are all walls with zero slip velocity. The inlet and outlet boundary conditions were defined to be mass flow at the inlet and pressure at the outlet. According to [fun09], this is the most robust option. At the sides of both the runner domain and draft tube domain a periodicity boundary condition has been used. This means that what goes out at one side enter the domain on the other side. This is assumed to be correct since the domains are repeating themselves on both sides.

The Shear Stress Transport model has been used as a turbulence model. This model works by using the $k - \omega$ at the wall and $k - \epsilon$ in the bulk flow[fun09].
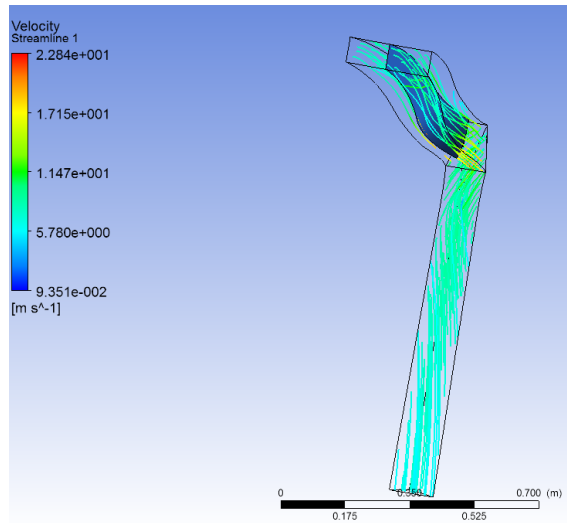
Figure 6.27: Streamlines in the runner and draft tube

Figure 6.27 and 6.28 shows the streamlines through the turbine. Since this is a best point simulation, the streamlines should go straight down in the draft tube domain. In figure 6.28 a higher relative velocity can be spotted at the turbine outlet, exactly as the calculations from Matlab predicted.
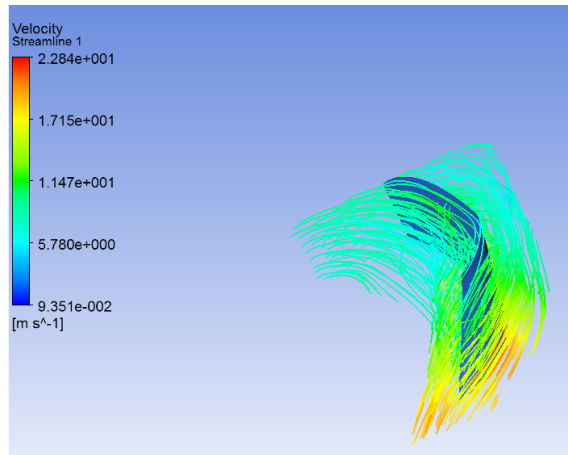
Figure 6.28: Velocity in the runner cascade
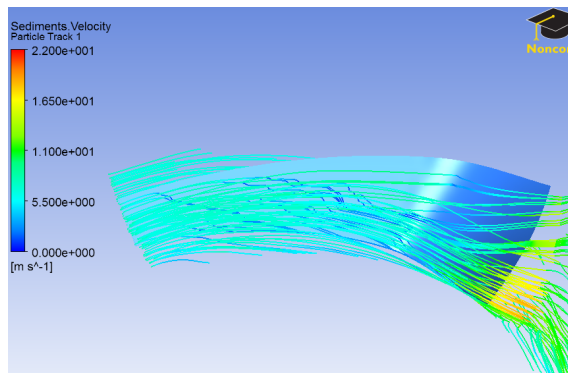
Figure 6.29: Particles through the runner cascade
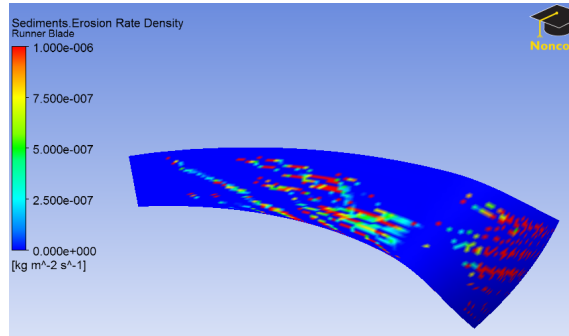
Figure 6.30: Erosion rate at runner's pressure side
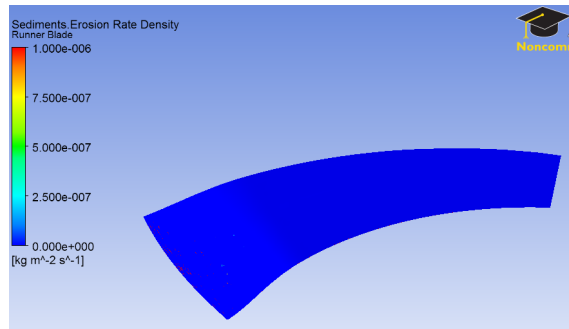
Figure 6.31: Erosion rate at runner's suction side

Figure 6.30 and 6.31 shows the erosion rate calculated in the CFD analysis. An obvious difference can be spotted between the two sides of the runner blade. The pressure side has the highest amount of erosion.

Chapter 7

Discussion

7.1   Runner Erosion

7.1.1   Outlet Angle

When trying to analyze the results from the erosion rate section, it can be useful to see how the relative velocity at both the inlet and outlet changes with respect to the outlet angle. This can be seen in figure 6.4. As derived in the theory section, see equation 4.5, we know that the outlet relative velocity has a bottom point at outlet angle that equals around 35 degrees. In the other end, the inlet relative velocity is almost linearly increasing with outlet angle, and has no bottom point, see equation 4.7.

These two issues make it difficult to find the outlet angle where the erosion rate is smallest. At least we can say that the outlet angle should never be higher than 35 degrees, because this will increase both inlet and outlet relative velocity, and hereby the average sediment erosion rate. As seen in figure 6.4, the sum of the two relative velocities has a bottom point at around 20 degrees. Due to this fact one may expect the erosion rate to be smallest here, and from the figures in the erosion rate section we see that this might be a good rule of thumb. As seen from the same figure, the outlet angle increase is less successful when the pole pair number is high. This is due to the fact that a high pole pair number gives a longer and thinner

runner, meaning that the inlet has more to say.

To sum up, it is not given what the outlet angle should be. From the theory section we know that the relative outlet velocity is smallest when the angle equals $\arctan \frac{1}{\sqrt{2}}$. On the other hand the average erosion rate of the turbine is likely to be smallest when the outlet angle is around 20-25 degrees. The chosen outlet angle should be between these two points. Which of the two features, minimal outlet erosion and minimal average erosion rate, you want to achieve will determine where.

7.1.2 Genetator Pole Number

When analyzing the figures of the erosion rate section, we see that by far the most efficient way to reduce the erosion is by increasing the number of pole pairs in the generator. This will make the runner rotate slower and by doing so decrease the radial component of the relative velocity. Since this component is dominating at the runner outlet, increasing the pole pair number will be especially effective in reducing the runner's outlet erosion. Doing so is very important since the erosion problem is greatest at this area. The gain from increasing the pole pair number is highest for the first number you add, and then becomes less and less. This was expected due to equation 3.4, which states that the rotation speed of the runner is reversely proportional to the pole pair number.

7.1.3 Reaction Degree

When dealing with the reaction degree, we clearly have to distinguish between two different cases. The easiest one is when the turbine doesn't have any guide vanes. When this is the case, the reaction degree should be 0.48 according to the erosion theory. When the turbine has guide vanes, the reaction degree should be higher in order to reduce erosion in the guide vanes. This is because a higher reaction degree means a lower absolute velocity through the guide vanes.

7.1.4   UCu distribution

As seen in the result section about the UCu distribution, this distribution
can heavily change the relative velocity through the runner.

When comparing figure 4.5, 6.12 and 6.14 we see that these different
distributions gives the runner quite different tangential component of the
relative velocity. The linear distribution gives the lowest relative velocity
of the three, because this distribution gives the waters absolute velocities
radial component a value closest to the tangential velocity of the runner.
Another finding is that the radial relative velocity can be both positive
and negative. Because of that and the fact that the relative velocity is
smallest if this component is zero, why not decide the UCu distribution by
the criteria that this component is zero? This is mathematically formulated
in equation 4.12. However, because of the no swirl criteria, this component
cannot be zero in the end of the runner. This is precisely why the Francis
runners tend to suffer from severe erosion at their outlet. This means that
our criteria for reducing sand erosion should be that the radial component
of the relative velocity equals zero as long as possible. See figure 6.16 where
both U and Cu have been plotted from a turbine designed according to that
criteria. This criteria will also give the runner a very special form, it will
not be curved as long as the radial component of the relative velocity equals
zero. The bended runner-end will reduce the absolute radial velocity of the
water to zero. This kind of runner also is easier to build, compared to more
curved runners.

7.1.5   All put together

Today's Jhimruk runner has an outlet angle equal to 18 degrees, and three
pole pairs[Yad04]. This means that the relative outlet velocity equals 31
m/s. This large velocity can be reduced by increasing both the outlet angle
and number of pole pairs. For example, by building a new turbine with
$\beta_2 = 25$ and Z=5, the outlet velocity is reduced to 20,7 m/s, and hereby
the outlet sand erosion by 70 percent. That is a radical change in the sand
erosion at the outlet, where the erosion problem in the runner is the biggest.

When testing Francis-runners with all possible combinations of the four different parameters discussed above, we should be able to see the whole picture. This result is shown in figure 6.17, 6.18 and 6.19, where the different figures represent different UCu distributions. The worst case is for the black distribution, see figure 6.9, and when looking at the different figures that plots both the waters radial velocity and the runners radial velocity, we clearly see why. In the red distribution, the absolute velocity's radial component follows the runners velocity much better, which gives a lower relative velocity throughout the runner. The best distribution is the distribution calculated for the criteria presented in the chapter: Velocity theory for Francis turbines. The differences are quite huge. The three pole pair's turbines have an erosion of around 3000 with the black distribution. To compare, the optimal distribution has around 1400. In other words, the erosion rate has been reduced by over 50 percent.

The range of erosion rate is stunning at the different runners that has been tested. From over 4000 at worst, to below 400 at the best. One reason is of course that the testing range for the different parameters has been large, maybe unrealistic.

7.1.6 Blade Area

In figure 6.20, the black line is telling that the area of the runner increases over 2.5 times when changing the pole pair number from three to seven. The reason for this increase is the fact that increasing the pole pair number also increases the inlet diameter. Since the axial view of the runner has form of an ellipsis, this will also increase the height difference between the inlet and outlet. The result is shown in figure 7.1.
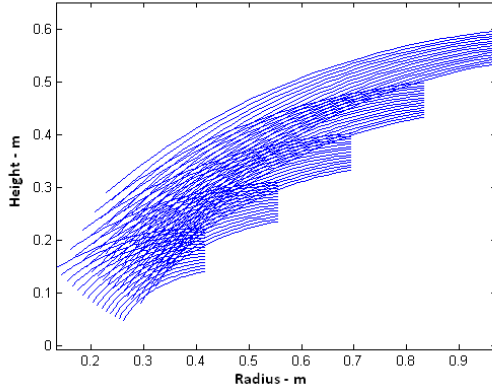
Figure 7.1: runners, with Z=3 - 7

Another change that affects the runner area is the UCu distribution. The more the runner is bended due to the UCu distribution, the bigger the area gets. The final design in this thesis is a straight line as long as possible, which makes it the most preferable when considering area.

As seen in figure 6.21, the area of the runner will be reduced when increasing the outlet angle. This is because an increase in outlet angle will decrease the inlet height of the runner, and thereby also the runner area.

7.2   Guide Vane Erosion

As seen in figure 6.23, the erosion in the guide vanes depend on all the three parameters that have been used troughout this thesis. These are the reaction degree, outlet angle and number of pole pairs. Not surprising, a higher reaction degree gives less erosion. The logic behind this finding can be seen in the following equation:

$$R = 1 - \frac{KineticEnergy}{TotalEnergy} \qquad [\text{-}] \qquad (7.1)$$

As the reaction degree is increased, the total amount of kinetic energy goes down. This means a lower velocity through the guide vanes and less erosion.

An increase in the pole pair number, gives a larger inlet diameter. This increases the circumference at the guide vane axis, which again increase the area. Since the flow rate is the same, this makes the velocity go down and thereby reduce the erosion.

We also see that the erosion goes down with higher outlet angle. This might seem a little strange at first, since a higher outlet angle gives a lower outlet diameter and hence a lower runner height at the inlet, which gives a lower inlet area and a higher velocity. This means that the erosion rate goes up, but since the height decreases the total erosion goes down. One should also notice that the axial velocity component we are talking about here is much less than the radial component.

7.3 Stay Vane Erosion

The only function of the stay vanes is to hold the spiral casing together. On the other side, stay vanes introduce two negative aspects. The friction between the vanes and the water adds some efficiency loss to the turbine. This loss will be increased if the stay vanes are exposed to sand erosion, because of the increased friction factor. The other aspect, when dealing with sand erosion, is the danger that one of the stay vanes will loosen from its position and travel through the runner. From a safety point of view this can be catastrophic. The worst case scenario is that this event will create a hole in the turbine, releasing a water leakage and floding the power house.

A solution to the two problems mentioned above, but still solving the problem the stay vanes are supposed to solve, is simply constructing the stay vanes at the outside of the spiral casing. Then we have reduced both the sand erosion and the friction loss of the stay vanes to zero. This solution is probably more expensive to build, but you will greatly increase the lifespan of the stay vanes.

When looking at the erosion at the stay vanes at different parameters, the same logic used in the discussion about the erosion in the guide vanes can be applied. Not strange since figure 6.23 and 6.24 looks almost identical. However, a difference in the two graphs is that the pole pair number doesn't seem to have such an impact on erosion as was the case in the guide vane cascade. This is due to the fact that since the diameter of the stay vanes is larger than that of the guide vanes, the relative change in diameter, and thereby the velocity, due to a change in number of pole pairs, is smaller than the case was for the guide vanes.

7.4 Friction

As stated in equation 4.13 the friction between the steel and the water, and thereby also the loss of energy, is proportional to the velocity squared. This means that another benefit from trying to reduce the velocity in order to reduce erosion also will help in reducing the energy loss due to friction. From figure 6.22, we see that the highest relative velocity between the water and the steel is by far greatest in the guide and stay vane cascade. This means that another good outcome from removing those cascades is the reduction of friction.

In the runner cascade, the changes in the parameter values made will make the runner larger. This increase will according to equation 4.13 proportionally increase the friction. However the changes made will also decrease the velocity in equation 4.13. This means that it is not certain that the friction loss has been increased by the new design. Another aspect is that since the sand erosion has been reduced, when time goes by the friction factor in equation 4.13 will not increase as much as before. This means that when the friction loss is integrated over time, the total energy loss will be less for the new design. This means that by addressing the sediment erosion in the turbine, the power plant will attain an economical improvement from two factors. The reduction in maintaining cost, and a higher efficiency that means more power production and thereby increased money income.

7.5 How will variations in flow and head change the sand erosion?

From the equations in the normal main dimensions, we find that the flow rate influences the number of poles. More water means more poles, and the speed of the runner goes down. As we have seen in the results section, an increase in the pole number is the most effective way to reduce the relative velocity through the runner, and in that way reduce the sand erosion. This means that there is a tendency of power plants with large flow rate to initially deal better with sand erosion. These power plants naturally have more poles in the generator, and it is at low water flow power plants that we have to increase the most the number of poles out of the normal number. The head will most of all decide the relative velocity in the runner inlet, and here the sand erosion is low already. Higher head means larger relative velocity. Higher head will also give a higher absolute velocity in the guide vanes and stay vanes. However, as suggested in this thesis, a solution might be to remove both these two rows of vanes.

7.6 Assumptions

When discussing the sediment erosion problem in this thesis, some assumptions have been made. In order to reflect over the validness of the results given, it will be necessary to evaluate these assumptions.

The first one is that the sediment particles follow the water flow. This doesn't need to be correct because the sediments and the water have different density, weight and other parameters that make them react different to the forces acting in the turbine. It is the relative velocity between the particles and the turbine that counts, not between the water and the turbine. However, since the particles at play here are so small and has so little mass, the assumption that the particles follow the water flow is acceptable.

The sediment erosion model that is used, is of course just a model. This means that it is a simplification of the real world. To validate the degree of accuracy of the model is considered outside the scope of this thesis.

7.7 Gear solution

Since one of the solutions to address sediment erosion is to increase the pole pair number, a gearbox solution should be mentioned. This is especially relevant when reducing erosion in existing power plants. To avoid buying a new generator but still get the benefit from a slower rotating runner, a gear may be placed between those two components. However, this will introduce mechanical losses and the cost of buying the gear box.

7.8 Simplification

When the Matlab code was made, one minor error was made for convenience reasons. That was to just remove some of the last points of the axial view in order to get the wanted shape of the runner end. This made the outlet diameter slightly bigger than it was meant to be. This error has found its way through all of my results. This was known the whole time, and did not change the essence of the results. However, if designing a runner in a water laden areas, this cutting should not be done that way since it will increase the radius and thereby the outlet erosion. This error is also why the bottom point of the graphs in figure 6.1 are changing a little bit, even though they shouldn't according to equation 4.5.

7.9 CFD

The CFD analysis performed in this thesis is mainly done with the intention that the author should gain some experience from CFD. Since the main focus in this thesis has been to find a better design of Francis turbines working in sediment laden water, there has been little time to test the design in a CFD analysis. The mesh is probably not good enough, and if time were sufficient, it would have been improved. The mesh quality is probably why the analysis failed to converged to the default residual criteria in the solver. In other words, the reader should understand that the CFD results are not presented as an absolute truth. However, some fundamental information

can be drawn from the analysis.

First and foremost, it seems like there is almost no swirl in the draft tube. This indicates that the design scripts from Matlab calculate a right runner curvature. Figure 6.28, with its higher velocity at the runner outlet, suggests that the relative velocity calculations from Matlab are valid.

The erosion at the runner's pressure side, shown in figure 6.30, seems to have a mismatch compared to figure 6.29 that track the sediment particle path. According to figure 6.29, it seems like the sediment erosion should be more present at the bottom outlet area because of a higher concentration of particles and higher particle velocity.

Chapter 8

Conclusion

Francis turbines suffer from sediment erosion in three different parts. These are the stay, guide and runner vanes.

A solution to the erosion problem in the stay vanes is to design them at the outside of the spiral casing instead of at the inside. By doing so, both the erosion and friction of the stay vanes drop to zero.

Two different possibilities have been presented to reduce the erosion in the guide vane cascade. One is to increase the reaction degree, but as seen in figure 6.23 also an increase in pole pair number and outlet angle will do. The other idea is to remove the guide vanes, and by doing so eliminating the whole erosion problem, and also reducing friction and stator-rotor interactions.

In order to reduce the erosion in the runner cascade, five different changes in the design have been suggested.
The most important thing is to increase the number of pole pairs in the generator. This is the most effective way of reducing the relative velocity at the runner outlet, where the erosion problem is biggest.
To decrease erosion in the runner, design the runner so the radial com-

ponent of the relative velocity, or equivalent, the difference between the runners speed and the waters radial velocity are as small as possible.

To reduce erosion at the inlet, the reaction degree should be equal to the hydraulic efficiency half.

If trying to reduce the erosion at the outlet to a minimum, the outlet angle should satisfy equation 4.5. However, the outlet angle that gives the lowest erosion rate will always be somewhat less.

Standard practice when designing Francis runners has been to cut off the runner-end. This should be reduced to a minimum in order to reduce erosion at the outlet. The logic behind this is that outlet erosion is proportional to the outlet radius cubed. If following these suggestions, the sediment erosion can be significantly reduced. When looking at the test case for this thesis, Jhimruk power plant, the outlet erosion has been reduced by around 70 percent and the overall erosion rate by around 50 percent. However, these improvements have a cost, and that is causd by a bigger turbine and generator.

Chapter 9

Future Work

- In this thesis, the blade doesn't have any thickness. The next step will be to test the blade with its thickness.

- When doing the CFD analysis, only the runner's best point has been tested. Therefore it is necessary to check how the new design behaves outside this optimum point. This has to be done through a new CFD analysis. One aspect of this work will be to compare these results to the runners in use today.

- Look at the possibilities to design a spherical valve that can open when the pressure difference over it is high, as is the case in high head Francis turbines.

- Study in depth the effect of changing the parameters value for the friction losses. This means analyzing how the friction factor will change over time due to sediment erosion, and thereby be able to calculate the increase in power production by addressing the erosion problem.

- The goal of this study has been to make water power in areas with a lot of sediments in the water more profitable. This means it is necessary to measure the economical gain of the new design compared to today's turbines. In order to do so, it will be necessary to relate

the numbers in the result part to how often the turbines have to be replaced. The gain in friction factor due to a less eroded surface has to be calculated, and related to an increase in turbine efficiency. When these things are done, the economical gain can be calculated through a net current investment value analysis.

Bibliography

[Bla07] Professor Olivier Blanchard. Macroeconomics. 2007.

[Bre03] Professor Hermod Brekke. Pumper og turbiner. Vannkraftlaboratoriet NTNU, 2003.

[Dah] Professor Ole Gunnar Dahlhaug. Personal pictures. Jhimruk power plant, Nepal.

[Elt09] Mette Eltvik. High pressure hydraulic machinery. 2009.

[Fra08] Håkon Hjort Francke. Konstruksjon av høytrykks francisturbiner. Ph.D student NTNU, 2008.

[fun09] Help function. Ansys cfx, realease 12.0. 2009.

[IEC09] IEC. Hydraulic machines – guide for dealing with abrasive erosion in water. 62364 Ed. 1.0, 2009.

[Neo10] Hari Prasad Neopane. Ph.d thesis. 2010.

[Pre] A BHEL Presentation. Latest trends in hydro turbine design. http://www.docstoc.com/docs/32582540/Latest-Trends-in-Hydro-Turbines.

[Tha10] Bhola Thapa. Sediment in nepalese hydropower projects. Kathamndu University, 2010.

[Whi08] Frank M. White. Fluid mechanics. Sixth Edition, 2008.

[Yad04] Ram Kumar Yadav. Design of francis turbine parts. Kathmandu University, 2004.
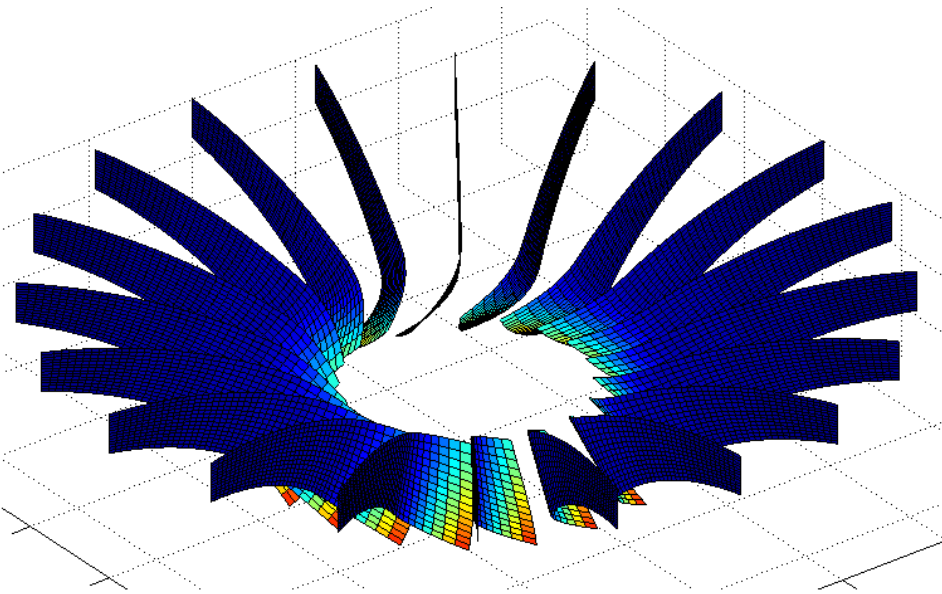
Appendix A

The New Jhimruk Design and CFD Mesh

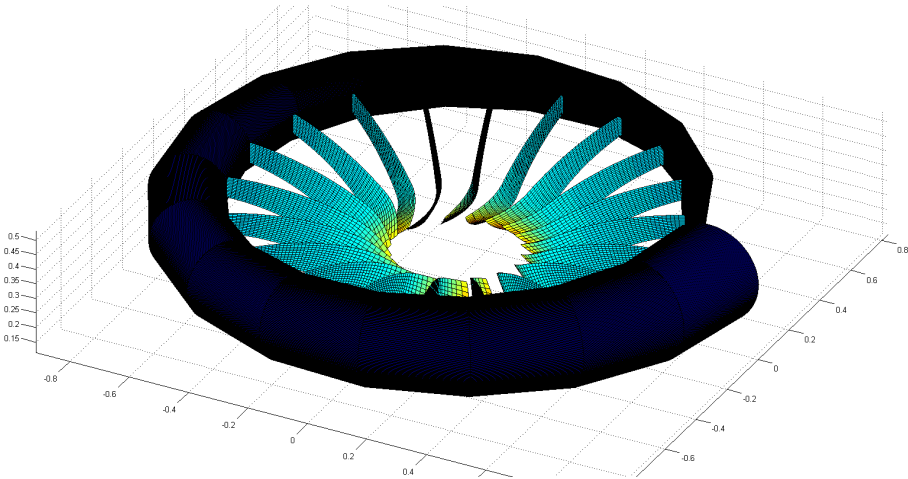Figure A.1: The New Runner Cascade

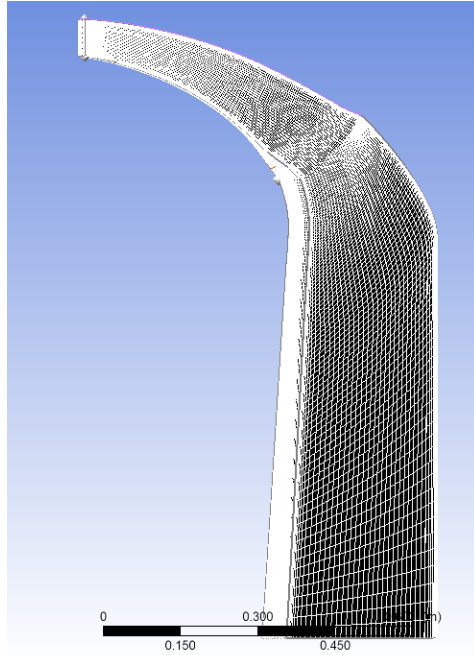Figure A.2: The New Runner Cascade with the spiral casing
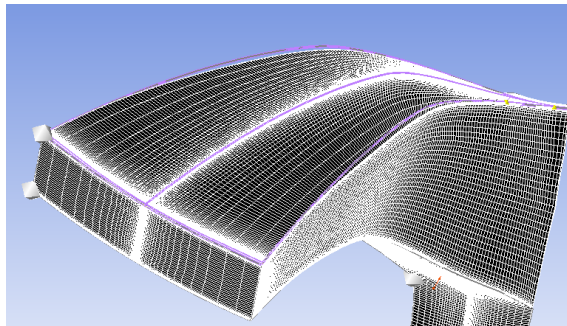
Figure A.3: The grid made from Turbogrid

Figure A.4: The grid made from Turbogrid at an different angle

Appendix B

CD

This CD contains the following:

- The Matlab-files used to design a turbine and test it for sediment erosion.

- The results presented in this thesis.